

Second-Kind Boundary Integral Equations for Electromagnetic Scattering at Composite Objects

X. Claeys and R. Hiptmair and E. Spindler

Research Report No. 2016-43
September 2016

Seminar für Angewandte Mathematik
Eidgenössische Technische Hochschule
CH-8092 Zürich
Switzerland

Second-Kind Boundary Integral Equations for Electromagnetic Scattering at Composite Objects

Xavier Claeys*, Ralf Hiptmair†,
and Elke Spindler†

September 30, 2016

Abstract We consider electromagnetic scattering of time-harmonic fields in \mathbb{R}^3 at objects composed of several linear, homogeneous, and isotropic materials. Adapting earlier work on acoustic scattering [X. CLAEYS, R. HIPTMAIR, AND E. SPINDLER, *A second-kind Galerkin boundary element method for scattering at composite objects*, BIT **55**(1):33–57, 2015] we develop a novel second-kind direct boundary integral formulation for this scattering problem, extending the so-called Müller formulation for a homogeneous scatterer to composite objects. The new formulation is amenable to Galerkin boundary element discretization by means of discontinuous tangential surface vector-fields. Numerical tests demonstrate competitive accuracy of the new approach compared with a widely used direct Galerkin boundary element method based on a first-kind boundary integral formulation. For piecewise constant approximation our experiments also confirm fast convergence of GMRES iterations independently of mesh resolution.

Keywords Electromagnetic scattering, second-kind boundary integral equations, Galerkin boundary element methods

Mathematics Subject Classification (2000) 65N12, 65N38, 65R20

* Sorbonne Universités, UPMC Univ Paris 06, CNRS, INRIA, UMR 7598, Laboratoire Jacques-Louis Lions, équipe Alpines, F-75005, Paris, France. The work of X.Claeys was partially supported the French National Research Agency under grant

† Seminar for Applied Mathematics, Swiss Federal Institute of Technology, Zurich, Switzerland, emails: {hiptmair,elke.spindler}@sam.math.ethz.ch. The work of E. Spindler was partially supported by SNF under grant 20021_137873/1.

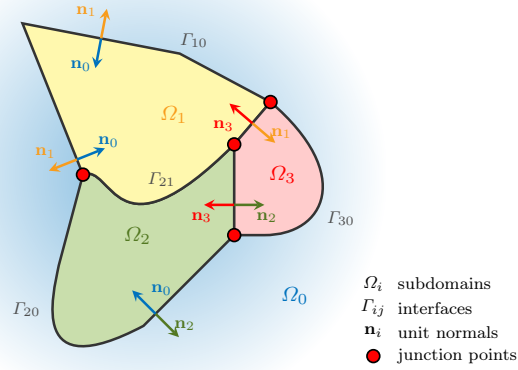


Fig. 1.1: Typical geometry of a cross section of a composite scatterer for $L = 3$.

1 Introduction

1.1 Model Problem for a Composite Scatterer

We consider scattering of an incident electromagnetic wave at an obstacle occupying the bounded region of space $\Omega_* \subset \mathbb{R}^3$. The obstacle is composed of several parts corresponding to open subdomains $\Omega_i \subset \Omega_*$, $i = 1, \dots, L$, that form a partition of Ω_* in the sense that $\Omega_i \cap \Omega_j = \emptyset$ for $j \neq i$ and $\overline{\Omega_*} = \bigcup_{i=1}^L \overline{\Omega_i}$. Both Ω_* and all Ω_i are supposed to be connected curvilinear Lipschitz polyhedra. This is also true of the unbounded complement $\Omega_0 := \mathbb{R}^3 \setminus \overline{\Omega_*}$. The generic situation that we have in mind is sketched in Figure 1.1. There, \mathbf{n}_i denotes the exterior unit normal vector field for Ω_i , $i = 1, \dots, L$. We denote the common interface of Ω_i and Ω_j by $\Gamma_{ij} = \partial\Omega_i \cap \partial\Omega_j$, $i \neq j$, $i, j \in \{1, \dots, L\}$. We call *skeleton* Σ the union of all interfaces Γ_{ij} : $\Sigma := \bigcup_{0 \leq j < i \leq L} \Gamma_{ij} = \bigcup_{i=0}^L \partial\Omega_i$.

The (lossless) materials of the parts of the scatterer and in Ω_0 possess different dielectric properties, reflected through different constant wave numbers $\kappa_i \in \mathbb{R}$, $i = 1, \dots, L$, prevailing in Ω_i . Defining a piecewise constant coefficient function $\kappa \in L^\infty(\mathbb{R}^3)$ by $\kappa|_{\Omega_i} := \kappa_i$, the total electric field \mathbf{E} will solve¹ (in a weak sense)

$$\mathbf{curl} \mathbf{curl} \mathbf{E} - \kappa(\mathbf{x})^2 \mathbf{E} = \mathbf{0} \quad \text{in } \mathbb{R}^3. \quad (1.1a)$$

¹ When referring to the composite, piecewise constant wave number, we are going write $\kappa(\mathbf{x})$ to emphasize the dependence of the wave number κ on $\mathbf{x} \in \mathbb{R}^d$.

In addition, the scattered field $\mathbf{E}_{\text{sc}} = \mathbf{E} - \mathbf{E}_{\text{inc}}$ must fulfill the Silver-Müller radiation conditions

$$\lim_{r \rightarrow \infty} \int_{\{\mathbf{x} \in \mathbb{R}^3 \mid \|\mathbf{x}\| = r\}} \left| \mathbf{curl} \mathbf{E}_{\text{sc}}(\mathbf{x}) \times \frac{\mathbf{x}}{r} - i\kappa_0 \mathbf{E}_{\text{sc}}(\mathbf{x}) \right|^2 dS(\mathbf{x}) = 0, \quad (1.1b)$$

where \mathbf{E}_{inc} denotes a given incident field satisfying (1.1a) for $\kappa(\mathbf{x}) \equiv \kappa_0$ in \mathbb{R}^3 . Existence and uniqueness of solutions of (1.1) is well established [23].

We point out that (1.1a) implies the following *transmission conditions* in the sense of distributions on Γ_{ij} for all $i, j \in \{0, \dots, L\}$, $i \neq j$:

$$\begin{aligned} (\mathbf{curl} \mathbf{E}_j)|_{\partial\Omega_j} \times \mathbf{n}_j + (\mathbf{curl} \mathbf{E}_i)|_{\partial\Omega_i} \times \mathbf{n}_i &= \mathbf{0}, \\ \mathbf{n}_j \times [\mathbf{E}_j|_{\partial\Omega_j} \times \mathbf{n}_j] - \mathbf{n}_i \times [\mathbf{E}_i|_{\partial\Omega_i} \times \mathbf{n}_i] &= \mathbf{0}, \end{aligned} \quad (1.2)$$

where we used the notation $\mathbf{E}_j := \mathbf{E}|_{\Omega_j}$, $j = 0, \dots, L$, and \mathbf{n}_i is the exterior unit normal for Ω_i , see Figure 1.1.

Remark 1.1 An important aspect in the setting of the composite scatterer is the presence of *material junction points and edges* (marked as \bullet in Figure 1.1), i.e. points and edges where three or more subdomains abut. In those regions some subdomains Ω_i will inevitably have non-smooth boundaries.

1.2 Boundary Integral Equations

To provide the foundation for a numerical treatment of the electromagnetic transmission problem (1.1) we transform it into *Boundary Integral Equations (BIEs)*. Among others, a rationale is that BIEs can easily accommodate unbounded domains, as long as the scatterer is bounded. Then we are going to use the *Galerkin Boundary Element Method (BEM)* to discretize the BIEs in variational form.

We will aim for a specific type of BIEs in variational form, so-called *single-trace* formulations (STF). The term *single-trace* refers to the class of *single-trace spaces*, on which the formulation is posed. *Single-trace spaces* are constructed in such a way that they contain the skeleton traces of all functions satisfying the *transmission conditions* (1.2). They will be defined precisely in Section 3.

The **first-kind single-trace formulation** is widely used and also known as Poggio-Miller-Chang-Harrington-Wu-Tsai (PMCHWT) scheme [11, 33, 39]. The formulation for a homogeneous scatterer ($L = 1$) was analyzed in [9, 10]. Its extension to composite obstacles is straightforward and is covered in [5]. Low-order Galerkin BEM for first-kind STFs yield ill-conditioned linear systems on fine meshes.

Nowadays, matrix compression techniques like *Adaptive Cross Approximation (ACA)* [2] or *Fast Multipole Methods (FMM)* [18, 34] are indispensable for competitive implementation of the BEM. They entail the use of iterative solvers. As a consequence, slow convergence of iterative solvers for

ill-conditioned Galerkin matrices becomes a major concern and preconditioning of the linear Galerkin systems arising from the first-kind STF becomes mandatory. Apparently, for composite scatterers with junction points/edges, the widely used so-called *Calderón preconditioning techniques* [25, 37] cannot be applied [14, Section 4], [15, Section 1]. It takes profound modifications of the integral equations in the form of so-called multi-trace formulations [14, 15], to pave the way for Calderón preconditioning.

In this article we pursue a different policy, the so-called **second-kind single-trace formulation**. In contrast to first-kind BIEs, low-order Galerkin BEM for second-kind boundary integral equations generally yield linear systems for which iterative solvers converge fast, rendering preconditioning unnecessary. For electromagnetic scattering at a homogeneous object ($L = 1$), second-kind BIEs are well-known, see [31, 38, 40], and they are sometimes called *Müller formulation*. For a long time it remained unclear how to extend them to composite scatterers, i.e. geometric arrangements that feature edges or points where more than two materials abut. Only recently, in [12, 17] and the parallel work [22], a breakthrough was achieved for acoustic transmission problems.

1.3 Novelty and Outline

Based on our work for acoustic scattering covered in [12, 16, 17] and the results for a homogeneous scatterer ($L = 1$) from [31, 38, 40], we extend the second-kind STF to composite electromagnetic scattering. In Section 2, we give a brief introduction to the relevant boundary integral equations. Appropriate spaces for boundary integral equations in the context of a composite scatterer, namely single- and multi-trace spaces, are explained in Subsection 3. In Subsection 4.2, we derive the second-kind STF based on a so-called *multi-potential* representation formula for the scattering solution, see Corollary 4.1.

Instead of working in classical energy trace spaces, in Subsection 4.3 we consider the second-kind STF in the space $\mathbf{L}_t^2(\Sigma)$ of square-integrable tangential vector fields on Σ . This is possible, because all the involved operators are continuous in $\mathbf{L}_t^2(\Sigma)$. The advantage of working in $\mathbf{L}_t^2(\Sigma)$ is, that it paves the way for switching to an interface-based variational formulation, see Section 4.4. It also provides more flexibility in choosing the trial and test spaces for Galerkin discretization, for instance, one may use simple piecewise constant vector fields on a given quasi-uniform and shape regular mesh of Σ , see Section 5.

Section 6 concludes the article with a presentation of numerical results, which indicate that the accuracy of the second-kind Galerkin solution can compete with the classical first-kind results. We observe that the spectra of the second-kind Galerkin matrices cluster around 1 and fast, almost mesh-independent convergence of GMRES.

2 Traces, Potentials and Boundary Integral Operators

On the boundary of Ω_i , we define the following space of *tangential, square integrable vector fields*:

$$\mathbf{L}_t^2(\partial\Omega_i) := \{ \mathbf{u} \in \mathbf{L}^2(\partial\Omega_i) : \mathbf{u} \cdot \mathbf{n}_i = 0 \text{ a.e. on } \partial\Omega_i \}. \quad (2.1)$$

It is endowed with the inner product $[\mathbf{u}, \mathbf{v}]_{\partial\Omega_i} := \langle \mathbf{u}, \bar{\mathbf{v}} \rangle_{\partial\Omega_i}$, where $\langle \mathbf{u}, \mathbf{v} \rangle_{\partial\Omega_i} := \int_{\partial\Omega_i} \mathbf{u} \cdot \mathbf{v} dS$.

Next we introduce *local* trace operators and potentials associated with a subdomain Ω_i , $i \in \{*, 0, 1, \dots, L\}$ and appropriate spaces on which the operators are well-defined. Writing $\mathcal{D}(\bar{\Omega}_i) := C_{\text{comp}}^\infty(\mathbb{R}^3)|_{\Omega_i}$ we define the local (interior) *tangential trace operators*

$$\begin{aligned} \gamma_\times^i : (\mathcal{D}(\bar{\Omega}_i))^3 &\rightarrow \mathbf{L}_t^2(\partial\Omega_i), & \mathbf{U} &\mapsto \mathbf{U} \times \mathbf{n}_i|_{\partial\Omega_i}, \\ \gamma_t^i : (\mathcal{D}(\bar{\Omega}_i))^3 &\rightarrow \mathbf{L}_t^2(\partial\Omega_i), & \mathbf{U} &\mapsto \mathbf{n}_i \times (\mathbf{U} \times \mathbf{n}_i)|_{\partial\Omega_i}. \end{aligned}$$

The presentation of BIEs for electromagnetic fields entails understanding the meaning of traces acting on functions in the “electromagnetic energy spaces”²

$$\begin{aligned} \mathbf{H}_{\text{loc}}(\mathbf{curl}^2, \Omega) &:= \{ \mathbf{U} \in \mathbf{H}_{\text{loc}}(\mathbf{curl}, \Omega) \mid \mathbf{curl} \mathbf{curl} \mathbf{U} \in \mathbf{L}_{\text{loc}}^2(\Omega) \}, \\ \mathbf{H}_{\text{loc}}(\mathbf{curl}, \Omega) &:= \{ \mathbf{U} \in \mathbf{L}_{\text{loc}}^2(\Omega) \mid \mathbf{curl} \mathbf{U} \in \mathbf{L}_{\text{loc}}^2(\Omega) \}. \end{aligned} \quad (2.2)$$

We are not going to give details and just recall some of the result from [4], borrowing all notations from that paper, among them the spaces

$$\begin{aligned} \mathbf{H}^{-\frac{1}{2}}(\mathbf{curl}_\Gamma, \partial\Omega_i) &:= \left\{ \mathbf{u} \in \mathbf{H}_\times^{-\frac{1}{2}}(\partial\Omega_i) : \mathbf{curl}_\Gamma \mathbf{u} \in \mathbf{H}^{-\frac{1}{2}}(\partial\Omega_i) \right\}, \\ \mathbf{H}^{-\frac{1}{2}}(\mathbf{div}_\Gamma, \partial\Omega_i) &:= \left\{ \mathbf{u} \in \mathbf{H}_t^{-\frac{1}{2}}(\partial\Omega_i) : \mathbf{div}_\Gamma \mathbf{u} \in \mathbf{H}^{-\frac{1}{2}}(\partial\Omega_i) \right\}, \end{aligned}$$

both endowed with the respective graph norms. We call them *electric and magnetic trace spaces* and use the shorthand notations $\mathcal{T}_{el}(\partial\Omega_i) := \mathbf{H}^{-\frac{1}{2}}(\mathbf{curl}_\Gamma, \partial\Omega_i)$ and $\mathcal{T}_m(\partial\Omega_i) := \mathbf{H}^{-\frac{1}{2}}(\mathbf{div}_\Gamma, \partial\Omega_i)$.

These two spaces are dual to each other when taking the extended the bilinear form $\langle \cdot, \cdot \rangle_{\partial\Omega_i}$ as duality pairing [6, p. 43]. For more information about the *surface divergence* \mathbf{div}_Γ and the *surface curl* \mathbf{curl}_Γ , we also refer to [8]. We summarize [6, Thm. 5.4], [8, Thm. 4.1] in the following trace theorem.

Lemma 2.1 (Electric and Magnetic Trace Operators) *The electric trace operator $\gamma_{el}^i := \gamma_t^i$ and magnetic trace operator $\gamma_m^i := \gamma_\times^i \circ \mathbf{curl}$ can be extended to bounded surjective mappings*

$$\gamma_{el}^i : \mathbf{H}_{\text{loc}}(\mathbf{curl}, \Omega_i) \rightarrow \mathcal{T}_{el}(\partial\Omega_i), \quad \gamma_m^i : \mathbf{H}_{\text{loc}}(\mathbf{curl}^2, \Omega_i) \rightarrow \mathcal{T}_m(\partial\Omega_i).$$

² The spaces $\mathbf{H}(\mathbf{curl}^2, \Omega)$, $\mathbf{H}(\mathbf{curl}, \Omega)$ are defined analogously by dropping the subscript *loc* everywhere in (2.2).

As a compact notation we use the *total energy trace space*

$$\mathcal{T}(\partial\Omega_i) := \mathcal{T}_{el}(\partial\Omega_i) \times \mathcal{T}_m(\partial\Omega_i), \quad (2.3)$$

which is *self-dual* with respect to the skew-symmetric pairing³

$$\langle\langle \mathbf{u}, \mathbf{v} \rangle\rangle_{\mathcal{T}(\partial\Omega_i)} := \langle \mathbf{u}, \boldsymbol{\varphi} \rangle_{\partial\Omega_i} - \langle \mathbf{v}, \boldsymbol{\nu} \rangle_{\partial\Omega_i}, \quad \mathbf{u} := \begin{pmatrix} \mathbf{u} \\ \boldsymbol{\nu} \end{pmatrix}, \quad \mathbf{v} := \begin{pmatrix} \mathbf{v} \\ \boldsymbol{\varphi} \end{pmatrix} \in \mathcal{T}(\partial\Omega_i).$$

A related compact notation is the *total trace operator* $\boldsymbol{\gamma}_{\text{tot}}^i$

$$\boldsymbol{\gamma}_{\text{tot}}^i : \mathbf{H}_{\text{loc}}(\mathbf{curl}^2, \Omega_i) \rightarrow \mathcal{T}(\partial\Omega_i), \quad \boldsymbol{\gamma}_{\text{tot}}^i \mathbf{U} := \begin{pmatrix} \gamma_{el}^i \mathbf{U} \\ \gamma_m^i \mathbf{U} \end{pmatrix}. \quad (2.4)$$

Next, we introduce local potentials associated with a subdomain Ω_i , $i \in \{*, 0, \dots, L\}$, see [9, Section 4], [10, Section 3.3], [27, Section 4.3]. For sufficiently regular scalar and vector valued functions on $\partial\Omega_i$, φ and $\boldsymbol{\varphi}$, respectively, the scalar and vector *single layer potentials* are given by the improper integrals

$$\begin{aligned} \mathbb{V}_i[\kappa](\varphi) &= \int_{\partial\Omega_i} \Phi_\kappa(\|\mathbf{x} - \mathbf{y}\|) \varphi(\mathbf{y}) dS(\mathbf{y}), \quad \mathbf{x} \in \mathbb{R}^3 \setminus \partial\Omega_i, \\ \mathbf{V}_i[\kappa](\boldsymbol{\varphi}) &= \int_{\partial\Omega_i} \Phi_\kappa(\|\mathbf{x} - \mathbf{y}\|) \boldsymbol{\varphi}(\mathbf{y}) dS(\mathbf{y}), \quad \mathbf{x} \in \mathbb{R}^3 \setminus \partial\Omega_i, \end{aligned} \quad (2.5)$$

based on the fundamental solution for the Helmholtz operator [35, Rem. 3.1.3]

$$\Phi_\kappa(\xi) = \frac{\exp(i\kappa\xi)}{4\pi\xi}, \quad \xi \in \mathbb{R} \setminus \{0\}. \quad (2.6)$$

For any $s \in (-\frac{1}{2}, \frac{1}{2}]$, they provide continuous linear operators [35, Sect. 3.1.2]

$$\begin{aligned} \mathbb{V}_i[\kappa] &: H^{s-\frac{1}{2}}(\partial\Omega_i) \rightarrow H_{\text{loc}}^{1+s}(\mathbb{R}^3 \setminus \partial\Omega_i), \\ \mathbf{V}_i[\kappa] &: \mathbf{H}^{s-\frac{1}{2}}(\partial\Omega_i) \rightarrow \mathbf{H}_{\text{loc}}^{1+s}(\mathbb{R}^3 \setminus \partial\Omega_i). \end{aligned}$$

These potentials enter the definition of the *Maxwell single and double layer potentials*

$$\mathbf{S}_i[\kappa](\boldsymbol{\varphi}) := \mathbf{V}_i[\kappa](\boldsymbol{\varphi}) + \frac{1}{\kappa^2} \mathbf{grad} \mathbb{V}_i[\kappa](\text{div}_\Gamma \boldsymbol{\varphi}), \quad (2.7)$$

$$\mathbf{D}_i[\kappa](\mathbf{v}) := \mathbf{curl} \mathbf{V}_i[\kappa](\mathbf{n}_i \times \mathbf{v}). \quad (2.8)$$

which give rise to continuous operators [9, Thm. 5]

$$\begin{aligned} \mathbf{S}_i[\kappa] &: \mathbf{H}^{-\frac{1}{2}}(\text{div}_\Gamma, \partial\Omega_i) \rightarrow \mathbf{H}_{\text{loc}}(\mathbf{curl}^2, \mathbb{R}^3 \setminus \partial\Omega_i) \cap \mathbf{H}_{\text{loc}}(\text{div } 0, \mathbb{R}^3 \setminus \partial\Omega_i), \\ \mathbf{D}_i[\kappa] &: \mathbf{H}^{-\frac{1}{2}}(\text{curl}_\Gamma, \partial\Omega_i) \rightarrow \mathbf{H}_{\text{loc}}(\mathbf{curl}^2, \mathbb{R}^3 \setminus \partial\Omega_i) \cap \mathbf{H}_{\text{loc}}(\text{div } 0, \mathbb{R}^3 \setminus \partial\Omega_i). \end{aligned}$$

³ Fraktur font is used to designate functions in the total energy trace space, whereas Roman typeface is reserved for electric traces, and Greek symbols for magnetic traces.

where

$$\mathbf{H}_{\text{loc}}(\text{div } 0, \mathbb{R}^3 \setminus \partial\Omega_i) := \{\mathbf{V} \in L_{\text{loc}}^2(\mathbb{R}^3) \mid \text{div } \mathbf{V} \equiv 0 \text{ on } \Omega_i \cup \mathbb{R}^3 \setminus \overline{\Omega}_i\}.$$

Moreover, the electric Maxwell single and double layer potentials supply solutions of the homogeneous Maxwell equation (1.1a) with constant wave number κ on $\Omega_i \cup \mathbb{R}^3 \setminus \overline{\Omega}_i$. They also satisfy the Silver-Müller radiation conditions (1.1b).

These potentials permit us to state the fundamental *Stratton-Chu representation formula*, which is the starting point for boundary integral equations for electromagnetic scattering, see [9, Theorem 6], [32, Theorem 5.5.1], [19, Section 6.2], [30, Section 9.2]:

Lemma 2.2 (Local Stratton-Chu Representation Formula)

Every solution $\mathbf{E} \in \mathbf{H}_{\text{loc}}(\text{curl}^2, \Omega_i) \cap \mathbf{H}_{\text{loc}}(\text{div } 0, \Omega_i)$ of $\text{curl } \text{curl } \mathbf{E} - \kappa^2 \mathbf{E} = \mathbf{0}$ in Ω_i (that satisfies the Silver-Müller radiation conditions, if $i = 0$,) fulfills

$$\mathbf{G}_i[\kappa](\boldsymbol{\gamma}_{\text{tot}}^i \mathbf{E}) = \begin{cases} \mathbf{E} & \text{on } \Omega_i, \\ \mathbf{0} & \text{on } \mathbb{R}^3 \setminus \overline{\Omega}_i, \end{cases}$$

where the local total potential is defined by

$$\mathbf{G}_i[\kappa](\mathbf{u}) := -\mathbf{D}_i[\kappa](\mathbf{u}) + \mathbf{S}_i[\kappa](\boldsymbol{\nu}), \quad \mathbf{u} := \begin{pmatrix} \mathbf{u} \\ \boldsymbol{\nu} \end{pmatrix} \in \mathcal{T}(\partial\Omega_i).$$

Off $\partial\Omega_i$ the potentials are regular enough to accommodate total traces from both sides of $\partial\Omega_i$. They satisfy the *jump relations* [9, Thm. 7]

$$(\boldsymbol{\gamma}_{\text{tot}}^{i,c} - \boldsymbol{\gamma}_{\text{tot}}^i) \mathbf{G}_i[\kappa](\mathbf{u}) = -\mathbf{u} \quad \text{for all } \mathbf{u} \in \mathcal{T}(\partial\Omega_i), \quad (2.9)$$

where $\boldsymbol{\gamma}_{\text{tot}}^{i,c}$ means the trace onto $\partial\Omega_i$ with normal vector field \mathbf{n}_i but taken from outside Ω_i (from inside its complement).

3 Multi- and Single-Trace Spaces

3.1 Energy Trace Spaces

The space containing all local traces of functions in $\mathbf{H}_{\text{loc}}(\text{curl}^2, \Omega_i)$, $i \in \{0, \dots, L\}$ is given by the *skeleton multi-trace space*, see also [13, Sections 3&4].

Definition 3.1 (Multi-Trace Space) The skeleton *multi-trace space* $\mathcal{MT}(\Sigma)$ is defined as the product of local total energy trace spaces from (2.3):

$$\mathcal{MT}(\Sigma) := \bigtimes_{i=0}^L \mathcal{T}(\partial\Omega_i) \cong \bigtimes_{i=0}^L \mathcal{T}_{el}(\partial\Omega_i) \times \bigtimes_{i=0}^L \mathcal{T}_m(\partial\Omega_i).$$

It owes its name to the fact that on each interface Γ_{ij} a function $\mathbf{u} \in \mathcal{MT}(\Sigma)$ comprises two pairs of electric and magnetic traces, one contributed by the subdomain on either side.

Next, we define the *skeleton multi-trace operator* $\gamma_{\text{tot}}^\Sigma$. It collects the total traces from (2.4) for all $i \in \{0, \dots, L\}$. Hence, it maps $\mathbf{H}_{\text{loc}}(\mathbf{curl}^2, \mathbb{R}^3 \setminus \Sigma)$ into the multi-trace space $\mathcal{MT}(\Sigma)$ and is given by

$$\gamma_{\text{tot}}^\Sigma : \begin{cases} \mathbf{H}_{\text{loc}}(\mathbf{curl}^2, \mathbb{R}^3 \setminus \Sigma) & \rightarrow \mathcal{MT}(\Sigma), \\ \mathbf{E} & \mapsto \gamma_{\text{tot}}^\Sigma \mathbf{E} := (\gamma_{\text{tot}}^0 \mathbf{E}, \dots, \gamma_{\text{tot}}^L \mathbf{E}). \end{cases} \quad (3.1)$$

Self-duality of $\mathcal{MT}(\Sigma)$ is induced by the \mathbf{L}_t^2 -type skew-symmetric bilinear pairing

$$\langle\langle \mathbf{u}, \mathbf{v} \rangle\rangle := \sum_{i=0}^L \langle\langle \mathbf{u}_i, \mathbf{v}_i \rangle\rangle_{\mathcal{T}(\partial\Omega_i)}, \quad \begin{aligned} \mathbf{u} &= (\mathbf{u}_0, \dots, \mathbf{u}_L) \\ \mathbf{v} &= (\mathbf{v}_0, \dots, \mathbf{v}_L) \end{aligned} \in \mathcal{MT}(\Sigma). \quad (3.2)$$

For sufficiently smooth functions we can rewrite (3.2) using the fact that each interface is visited twice when summing integrals over all subdomain boundaries:

$$\langle\langle \mathbf{u}, \mathbf{v} \rangle\rangle = \sum_{0 \leq j < i \leq L} \int_{\Gamma_{ij}} \mathbf{u}_i \cdot \boldsymbol{\nu}_i - \boldsymbol{\nu}_i \cdot \mathbf{v}_i + \mathbf{u}_j \cdot \boldsymbol{\varphi}_j - \boldsymbol{\nu}_j \cdot \mathbf{v}_j \, dS, \quad (3.3)$$

where we used the notation $\mathbf{u}_i = (\mathbf{u}_i, \boldsymbol{\nu}_i)$, $\mathbf{v}_i = (\mathbf{v}_i, \boldsymbol{\varphi}_i)$ for $\mathbf{u}_i, \mathbf{v}_i \in \mathcal{T}(\partial\Omega_i)$ from (3.2).

We introduce the subspace of $\mathcal{MT}(\Sigma)$ compatible with the transmission conditions (1.2).

Definition 3.2 (Skeleton Single-Trace Space) The *skeleton single-trace space* $\mathcal{ST}(\Sigma)$ is defined as

$$\mathcal{ST}(\Sigma) := \left\{ ((\mathbf{u}_0, \boldsymbol{\nu}_0), \dots, (\mathbf{u}_L, \boldsymbol{\nu}_L)) \in \mathcal{MT}(\Sigma) \mid \exists \mathbf{U} \in \mathbf{H}(\mathbf{curl}, \mathbb{R}^3) \right. \\ \left. \mathbf{u}_i = \gamma_t^i \mathbf{U}, \exists \mathbf{V} \in \mathbf{H}(\mathbf{curl}, \mathbb{R}^3), \boldsymbol{\nu}_i = \gamma_\times^i \mathbf{V}, \forall i \in \{0, \dots, L\} \right\}.$$

The skeleton single-trace space collects all possible skeleton multi-traces of solutions of (1.1a) in $\mathcal{MT}(\Sigma)$:

$$\mathbf{E} \text{ solves (1.1)} \quad \Rightarrow \quad \gamma_{\text{tot}}^\Sigma \mathbf{E} \in \mathcal{ST}(\Sigma). \quad (3.4)$$

The following *polar set* characterization of $\mathcal{ST}(\Sigma)$ as a subspace of $\mathcal{MT}(\Sigma)$, see also [13, Prop. 3.1], [14, Thm. 3.1], will play an important role when deriving the single-trace formulations.

Lemma 3.1 (Polarity Property) *The single-trace space $\mathcal{ST}(\Sigma)$ is a Lagrangian subspace of $\mathcal{MT}(\Sigma)$*

$$\mathcal{ST}(\Sigma) = \{ \mathbf{u} \in \mathcal{MT}(\Sigma) : \langle\langle \mathbf{u}, \mathbf{v} \rangle\rangle = 0, \forall \mathbf{v} \in \mathcal{ST}(\Sigma) \}.$$

The proof uses the same ideas as used to verify [12, Proposition 2.1] in the acoustic setting. As an immediate corollary, the single-trace space is closed in $\mathcal{MT}(\Sigma)$.

3.2 \mathbf{L}_t^2 trace spaces

Since we aim for formulations in \mathbf{L}_t^2 , we need \mathbf{L}_t^2 -counterparts of the spaces from the previous subsection.

Definition 3.3 (\mathbf{L}_t^2 -Multi-Trace Space) The *skeleton \mathbf{L}_t^2 -multi-trace space* $\mathcal{ML}_t(\Sigma)$ is the Hilbert space

$$\mathcal{ML}_t(\Sigma) := \prod_{i=0}^L (\mathbf{L}_t^2(\partial\Omega_i) \times \mathbf{L}_t^2(\partial\Omega_i)) \cong \left(\prod_{i=0}^L \mathbf{L}_t^2(\partial\Omega_i) \right) \times \left(\prod_{i=0}^L \mathbf{L}_t^2(\partial\Omega_i) \right).$$

The bilinear pairing from (3.2) extends naturally to the \mathbf{L}_t^2 -setting. Moreover, in contrast to the classical energy trace setting, the restriction operator to an interface Γ_{ij} is well defined in $\mathcal{ML}_t(\Sigma)$. Hence, on $\mathcal{ML}_t(\Sigma)$ we can redefine (3.2) as follows.

$$\langle\langle \mathbf{u}, \mathbf{v} \rangle\rangle = \sum_{j < i} \int_{\Gamma_{ij}} \mathbf{u}_i \cdot \boldsymbol{\varphi}_i - \boldsymbol{\nu}_i \cdot \mathbf{v}_i + \mathbf{u}_j \cdot \boldsymbol{\varphi}_j - \boldsymbol{\nu}_j \cdot \mathbf{v}_j \, dS, \quad (3.5)$$

with $\mathbf{u} = (\mathbf{u}_0, \dots, \mathbf{u}_L)$, $\mathbf{u}_i = (\mathbf{u}_i, \boldsymbol{\nu}_i) \in \mathbf{L}_t^2(\partial\Omega_i) \times \mathbf{L}_t^2(\partial\Omega_i)$ and $\mathbf{v} = (\mathbf{v}_0, \dots, \mathbf{v}_L)$, $\mathbf{v}_i = (\mathbf{v}_i, \boldsymbol{\varphi}_i) \in \mathbf{L}_t^2(\partial\Omega_i) \times \mathbf{L}_t^2(\partial\Omega_i)$, $i \in \{0, \dots, L\}$.

The subspace of functions in $\mathcal{ML}_t(\Sigma)$ complying with the transmission conditions (1.2), i.e. the analogue to the classical single-trace space $\mathcal{ST}(\Sigma)$, can be defined as follows:

Definition 3.4 (\mathbf{L}_t^2 -Single-Trace Space) The *\mathbf{L}_t^2 -single-trace space* $\mathcal{SL}_t(\Sigma)$ is given by

$$\mathcal{SL}_t(\Sigma) := \left\{ \left(\begin{pmatrix} \mathbf{u}_0 \\ \boldsymbol{\nu}_0 \end{pmatrix}, \dots, \begin{pmatrix} \mathbf{u}_L \\ \boldsymbol{\nu}_L \end{pmatrix} \right) \in \mathcal{ML}_t(\Sigma) \mid \mathbf{u}_j|_{\Gamma_{ij}} = \mathbf{u}_i|_{\Gamma_{ij}}, \boldsymbol{\nu}_j|_{\Gamma_{ij}} = -\boldsymbol{\nu}_i|_{\Gamma_{ij}} \quad \forall j < i \in \{0, \dots, L\} \right\}.$$

Note that the constraints in Definition 3.4 encode the transmission conditions (1.2).

As in the case of the classical single-trace space $\mathcal{ST}(\Sigma)$, there is a Lagrangian subspace characterization of $\mathcal{SL}_t(\Sigma)$ as a subspace of $\mathcal{ML}_t(\Sigma)$:

Lemma 3.2 (Polarity Property) The *\mathbf{L}_t^2 -single-trace space $\mathcal{SL}_t(\Sigma)$ can be identified as its own polar set in the \mathbf{L}_t^2 -multi-trace space $\mathcal{ML}_t(\Sigma)$*

$$\mathcal{SL}_t(\Sigma) = \{ \mathbf{u} \in \mathcal{ML}_t(\Sigma) : \langle\langle \mathbf{u}, \mathbf{v} \rangle\rangle = 0, \forall \mathbf{v} \in \mathcal{SL}_t(\Sigma) \}.$$

The proof is analogous to the one from [17, Lemma 4.1], see also [36, Lem. 6.2.7]. Again, it is immediate that $\mathcal{SL}_t(\Sigma) \subset \mathcal{ML}_t(\Sigma)$ is closed.

4 Second-Kind Single-Trace Formulation

4.1 Preface: Homogeneous Scatterer $L = 1$

For the case $L = 1$, that is, a simple homogeneous scatterer, there is only a single interface $\Gamma_{01} = \partial\Omega_0 = \partial\Omega_1$. In this setting the second-kind Müller formulation is well known [31, § 23], but we recall it to fix ideas and guide the reader gently towards our generalization derived in the next two subsections. Lemma 2.2 provides the following potential representation for the solution \mathbf{E} of (1.1):

$$\mathbf{E} = \begin{cases} \mathbf{E}_{\text{inc}} - \mathbf{D}_0[\kappa_0](\gamma_{el}^0(\mathbf{E} - \mathbf{E}_{\text{inc}})) + \mathbf{S}_0[\kappa_0](\gamma_m^0(\mathbf{E} - \mathbf{E}_{\text{inc}})) & \text{in } \Omega_0, \\ -\mathbf{D}_1[\kappa_1](\gamma_{el}^1 \mathbf{E}) + \mathbf{S}_1[\kappa_1](\gamma_m^1 \mathbf{E}) & \text{in } \Omega_1. \end{cases} \quad (4.1)$$

To streamline notations, we write $\{\gamma\}_\Gamma$ for the arithmetic average of interior and exterior traces onto $\Gamma := \Gamma_{01}$ for some trace operator γ . For instance, $\{\gamma_{el}\}_\Gamma$ returns the average of the electric trace for a vectorfield defined on both sides of Γ . Moreover, we write $\gamma_{\mathbf{x}}$ for the pointwise restriction of a function to Γ . Taking electric and magnetic traces of \mathbf{E} onto Γ from both sides, using the definition (2.7) of $\mathbf{S}_i[\kappa]$, the identity $\gamma_m^i \mathbf{D}_i[\kappa](\mathbf{v}) = \kappa^2 \gamma_{\times}^i \mathbf{V}_i[\kappa](\mathbf{n}_i \times \mathbf{v}) - \mathbf{curl}_\Gamma \mathbb{V}_i[\kappa](\mathbf{curl}_\Gamma \mathbf{v})$ [24, Lemma 5.3], and applying the jump relations (2.9) yields boundary integral equations:

$$\begin{aligned} \gamma_{el}^1 \mathbf{E} &= -\{\gamma_{el}\}_\Gamma \mathbf{D}_1[\kappa_1](\gamma_{el}^1 \mathbf{E}) + \frac{1}{2} \gamma_{el}^1 \mathbf{E} + \{\gamma_{el}\}_\Gamma \mathbf{V}_1[\kappa_1](\gamma_m^1 \mathbf{E}) \\ &\quad + \kappa_1^{-2} \mathbf{grad}_\Gamma \{\gamma_{\mathbf{x}}\}_\Gamma \mathbb{V}_1[\kappa_1](\text{div}_\Gamma(\gamma_m^1 \mathbf{E})), \\ \gamma_m^1 \mathbf{E} &= +\mathbf{curl}_\Gamma \{\gamma_{\mathbf{x}}\}_\Gamma \mathbb{V}_1[\kappa_1](\text{curl}_\Gamma(\gamma_{el}^1 \mathbf{E})) + \kappa_1^2 \{\gamma_{\times}\}_\Gamma \mathbf{V}_1[\kappa_1](\gamma_{el}^1 \mathbf{E} \times \mathbf{n}_1) \\ &\quad + \{\gamma_m^1\}_\Gamma \mathbf{V}_1[\kappa_1](\gamma_m^1 \mathbf{E}) + \frac{1}{2} \gamma_m^1 \mathbf{E}, \\ \gamma_{el}^0 \mathbf{E} &= -\{\gamma_{el}\}_\Gamma \mathbf{D}_0[\kappa_0](\gamma_{el}^0 \mathbf{E}) + \frac{1}{2} \gamma_{el}^0 \mathbf{E} + \{\gamma_{el}\}_\Gamma \mathbf{V}_0[\kappa_0](\gamma_m^0 \mathbf{E}) \\ &\quad + \kappa_0^{-2} \mathbf{grad}_\Gamma \{\gamma_{\mathbf{x}}\}_\Gamma \mathbb{V}_0[\kappa_0](\text{div}_\Gamma(\gamma_m^0 \mathbf{E})) + \dots, \\ \gamma_m^0 \mathbf{E} &= +\mathbf{curl}_\Gamma \{\gamma_{\mathbf{x}}\}_\Gamma \mathbb{V}_0[\kappa_0](\text{curl}_\Gamma(\gamma_{el}^0 \mathbf{E})) + \kappa_0^2 \{\gamma_{\times}\}_\Gamma \mathbf{V}_0[\kappa_0](\gamma_{el}^0 \mathbf{E} \times \mathbf{n}_0) \\ &\quad + \{\gamma_m^0\}_\Gamma \mathbf{V}_0[\kappa_0](\gamma_m^0 \mathbf{E}) + \frac{1}{2} \gamma_m^0 \mathbf{E} + \dots \end{aligned}$$

Here the ellipsis \dots stands for terms involving \mathbf{E}_{inc} , which we do not state for the sake of clarity. They will enter the right hand sides of the boundary integral equations. Below we specify them for the general formulation. Notice that by the transmission conditions $\gamma_{el}^1 \mathbf{E} = \gamma_{el}^0 \mathbf{E}$ and $\gamma_m^1 \mathbf{E} = -\gamma_m^0 \mathbf{E}$. We use this fact and add the electric traces, weighted with κ_i^2 :

$$\begin{aligned} \frac{1}{2} (\kappa_1^2 + \kappa_0^2) \gamma_{el}^1 \mathbf{E} &= -\{\gamma_{el}\}_\Gamma (\kappa_1^2 \mathbf{D}_1[\kappa_1] - \kappa_0^2 \mathbf{D}_0[\kappa_0])(\gamma_{el}^1 \mathbf{E}) \\ &\quad + \{\gamma_{el}\}_\Gamma (\kappa_1^2 \mathbf{V}_1[\kappa_1] - \kappa_0^2 \mathbf{V}_0[\kappa_0])(\gamma_m^1 \mathbf{E}) \\ &\quad + \mathbf{grad}_\Gamma \{\gamma_{\mathbf{x}}\}_\Gamma (\mathbb{V}_1[\kappa_1] - \mathbb{V}_0[\kappa_0])(\text{div}_\Gamma(\gamma_m^1 \mathbf{E})) + \dots \end{aligned} \quad (4.2a)$$

Note that $\mathbf{D}_0[\kappa] = -\mathbf{D}_1[\kappa]$ due to the opposite orientation of normals. We can also subtract the magnetic traces and get

$$\begin{aligned} \gamma_m^1 \mathbf{E} = & + \mathbf{curl}_\Gamma \{ \gamma_{\mathbf{x}} \}_\Gamma (\mathbf{V}_1[\kappa_1] - \mathbf{V}_1[\kappa_0]) (\mathbf{curl}_\Gamma (\gamma_{el}^1 \mathbf{E})) \\ & + \{ \gamma_{\times} \}_\Gamma (\kappa_1^2 \mathbf{V}_1[\kappa_1] - \kappa_0^2 \mathbf{V}_1[\kappa_0]) (\gamma_{el}^1 \mathbf{E} \times \mathbf{n}_1) \\ & + \{ \gamma_m^1 \}_\Gamma (\mathbf{V}_1[\kappa_1] - \mathbf{V}_1[\kappa_0]) (\gamma_m^1 \mathbf{E}) + \dots \end{aligned} \quad (4.2b)$$

Thus, we arrive at two boundary integral equations for the two unknown traces $\gamma_{el}^1 \mathbf{E}$ and $\gamma_m^1 \mathbf{E}$. Yet, the key benefit of the above special linear combinations is that they lead to differences of single layer potentials that differ in wave number only, marked with **red** in (4.2). There cancellation of the leading singularities of their integral kernels will occur. Thus, the difference potentials will be strongly regularizing. More precisely, according to [35, Lemma 3.9.8], they map continuously $H^{-1}(\partial\Omega_i) \rightarrow H_{loc}^{\frac{5}{2}}(\mathbb{R}^3 \setminus \partial\Omega_i)$ in both the scalar and vectorial case.

We conclude that the boundary integral operators in the third line of (4.2a) and the first and third line of (4.2b) will be bounded and even *compact* in $\mathbf{L}_t^2(\Gamma)$. The same holds true for the vectorial single layer boundary integral operators highlighted in **green** in (4.2). Moreover, as explained in [9, Lemma 11], for any κ the boundary integral operators $\{ \gamma_{el} \}_\Gamma \mathbf{D}_1[\kappa]$ (printed in **blue** in (4.2)) feature Cauchy-singular kernels and are continuous in $\mathbf{L}_t^2(\Gamma)$. If Γ is smooth, they will even turn out to be compact in that space. Summing up, (4.2) can be rescaled to the form $(\text{Id} - \mathbf{T}) \begin{pmatrix} \gamma_{el}^1 \mathbf{E} \\ \gamma_m^1 \mathbf{E} \end{pmatrix} = \dots$ with \mathbf{T} continuous on $\mathbf{L}_t^2(\Gamma) \times \mathbf{L}_t^2(\Gamma)$, a typical 2nd-kind boundary integral equation.

Remark 4.1 (Fredholmness of Index Zero) The integral operator \mathbf{T} underlying (4.2) is Fredholm of index zero in $\mathbf{L}_t^2(\Gamma) \times \mathbf{L}_t^2(\Gamma)$, see [38, Lemma 4.1], [38, Lemma 4.6] (for the case of a C^1 -domain), and [28, p. 155ff., ‘‘An alternative proof of xix in Theorem 5.1’’] or [29, Theorem 1.1] for merely Lipschitz Γ . Since uniqueness of solutions of (4.2) can be established by standard arguments, existence of a solution in $\mathbf{L}_t^2(\Gamma) \times \mathbf{L}_t^2(\Gamma)$ is guaranteed and it will supply the traces $(\gamma_{el}^1 \mathbf{E}, \gamma_m^1 \mathbf{E})$.

4.2 Second-Kind Formulation in Energy Trace Spaces

For $L > 1$ the key idea underlying the derivation of the second-kind single-trace formulation is a multi-potential representation formula. For acoustic scattering this was given in [17, Def. 3.3]. For electromagnetics an additional judicious scaling is needed in order to cope with the division by κ^2 in the Maxwell single layer potential $\mathbf{S}_i[\kappa]$ from (2.7).

Definition 4.1 (Scaled Multi-Potential) The *Maxwell multi-potential* is defined as the sum of *all* (possibly scaled) local potentials $\mathbf{G}_i[\kappa_i]$, $i = 0, \dots, L$:

$$\mathbf{M}[\boldsymbol{\theta}, \boldsymbol{\alpha}] : \begin{cases} \mathcal{MT}(\Sigma) & \rightarrow \mathbf{H}_{loc}(\mathbf{curl}^2, \mathbb{R}^3 \setminus \Sigma), \\ \mathbf{u} = (\mathbf{u}_0, \dots, \mathbf{u}_L) & \mapsto \sum_{i=0}^L \alpha_i^2 \mathbf{G}_i[\theta_i](\mathbf{u}_i), \end{cases}$$

with $\boldsymbol{\theta} := (\theta_0, \dots, \theta_L) \in \mathbb{R}_+^{L+1}$ representing a *wave number vector* and $\boldsymbol{\alpha} = (\alpha_0, \dots, \alpha_L) \in \mathbb{R}^{L+1}$ a *scaling parameter vector*.

The special wave number vector $\boldsymbol{\kappa}$ collects the given wave numbers prevailing in the subdomains: $\boldsymbol{\kappa} = (\kappa_0, \dots, \kappa_L)$. Then, an immediate consequence of the local Stratton-Chu representation formula from Lemma 2.2 is the following.

Corollary 4.1 (Global Representation Formula) *A solution \mathbf{E} of the transmission problem (1.1) satisfies for any $\boldsymbol{\alpha} \in \mathbb{R}_+^{L+1}$*

$$\sum_{i=0}^L \alpha_i^2 \chi_{\Omega_i} \mathbf{E} - \alpha_0^2 \chi_{\Omega_0} \mathbf{E}_{\text{inc}} = \mathbf{M}[\boldsymbol{\kappa}, \boldsymbol{\alpha}] \boldsymbol{\gamma}_{\text{tot}}^\Sigma (\mathbf{E} - \chi_{\Omega_0} \mathbf{E}_{\text{inc}}), \quad (4.3)$$

where χ_Ω stands for the characteristic function of a domain Ω .

Corollary 4.1 provides the starting point for the derivation of the second-kind BIE for composite scatterers. Taking the cue from the linear combination used in Section 4.1, we fix the scaling parameter vector to be $\boldsymbol{\alpha} = \boldsymbol{\kappa}$ when taking the electric trace and use $\boldsymbol{\alpha} = \mathbf{1} := (1, \dots, 1)$ in the case of the magnetic trace. To keep notations short, we introduce the *global compound boundary integral operator* $\mathbf{M}[\boldsymbol{\theta}]$ for any $\boldsymbol{\theta} \in \mathbb{R}_+^{L+1}$ by

$$\mathbf{M}[\boldsymbol{\theta}] : \begin{cases} \mathcal{MT}(\Sigma) \rightarrow \mathcal{MT}(\Sigma), \\ \mathbf{u} \mapsto \begin{pmatrix} \gamma_{el}^\Sigma \mathbf{M}[\boldsymbol{\theta}, \boldsymbol{\theta}](\mathbf{u}) \\ \gamma_m^\Sigma \mathbf{M}[\boldsymbol{\theta}, \mathbf{1}](\mathbf{u}) \end{pmatrix}, \end{cases} \quad (4.4)$$

where $\gamma_{el}^\Sigma \mathbf{U} := (\gamma_{el}^0 \mathbf{U}, \dots, \gamma_{el}^L \mathbf{U})$, $\gamma_m^\Sigma \mathbf{U} := (\gamma_m^0 \mathbf{U}, \dots, \gamma_m^L \mathbf{U})$. Taking the skeleton multi-trace $\boldsymbol{\gamma}_{\text{tot}}^\Sigma$ on both sides of the global representation formula from Corollary 4.1, we obtain

$$(\mathbf{Id}_\kappa - \mathbf{M}[\boldsymbol{\kappa}]) \boldsymbol{\gamma}_{\text{tot}}^\Sigma \mathbf{E} = (\mathbf{Id}_\kappa - \mathbf{M}[\boldsymbol{\kappa}]) \boldsymbol{\epsilon}_{\text{inc},0}, \quad (4.5)$$

where the scaling operator $\mathbf{Id}_\kappa : \mathcal{MT}(\Sigma) \rightarrow \mathcal{MT}(\Sigma)$ is defined as

$$\mathbf{Id}_\kappa \left(\begin{pmatrix} \mathbf{v}_0 \\ \phi_0 \end{pmatrix}, \dots, \begin{pmatrix} \mathbf{v}_L \\ \phi_L \end{pmatrix} \right) := \left(\begin{pmatrix} \kappa_0^2 \mathbf{v}_0 \\ \phi_0 \end{pmatrix}, \dots, \begin{pmatrix} \kappa_L^2 \mathbf{v}_L \\ \phi_L \end{pmatrix} \right) \quad (4.6)$$

and $\boldsymbol{\epsilon}_{\text{inc},0} := (\boldsymbol{\gamma}_{\text{tot}}^0 \mathbf{E}_{\text{inc}}, \mathbf{0}, \dots, \mathbf{0})$.

Remark 4.2 (Notation) in the sequel, for the sake of brevity, we write \mathbf{M} and \mathbf{M} instead of $\mathbf{M}[\boldsymbol{\kappa}, \boldsymbol{\kappa}]$ and $\mathbf{M}[\boldsymbol{\kappa}]$. When we refer to a setting where all $L+1$ wave numbers are equal to $\theta \in \mathbb{R}_+$ and all scaling coefficients agree with $\alpha \in \mathbb{R}$, we write $\mathbf{M}[\boldsymbol{\theta}, \boldsymbol{\alpha}] = \mathbf{M}[(\theta, \dots, \theta), (\alpha, \dots, \alpha)]$ and $\mathbf{M}[\boldsymbol{\theta}] = \mathbf{M}[(\theta, \dots, \theta)]$.

Remark 4.3 (Right-hand Side) By assumption, \mathbf{E}_{inc} solves the electromagnetic scattering problem in $\Omega_* = \mathbb{R}^3 \setminus \overline{\Omega}_0$ for $\kappa = \kappa_0$. Hence, we obtain from the Stratton-Chu local representation formula from Lemma 2.2 that

$$\mathbf{G}_*[\kappa_0]\{\boldsymbol{\gamma}_{\text{tot}}^* \mathbf{E}_{\text{inc}}\} = \begin{cases} \mathbf{E}_{\text{inc}} & \text{on } \Omega_* = \mathbb{R}^3 \setminus \overline{\Omega}_0, \\ \mathbf{0} & \text{on } \Omega_0. \end{cases} \quad (4.7)$$

Since $\mathbf{E}_{\text{inc}} \in \mathbf{H}_{\text{loc}}(\mathbf{curl}^2, \mathbb{R}^3)$, it holds that $(\boldsymbol{\gamma}_{\text{tot}}^{0,c} - \boldsymbol{\gamma}_{\text{tot}}^0) \mathbf{E}_{\text{inc}} = \mathbf{0}$, which means, since $\Omega_* = \mathbb{R}^3 \setminus \overline{\Omega}_0$,

$$\boldsymbol{\gamma}_{\text{el}}^* \mathbf{E}_{\text{inc}} = \boldsymbol{\gamma}_{\text{el}}^0 \mathbf{E}_{\text{inc}} \quad , \quad \boldsymbol{\gamma}_m^* \mathbf{E}_{\text{inc}} = -\boldsymbol{\gamma}_m^0 \mathbf{E}_{\text{inc}}. \quad (4.8)$$

Hence we can rewrite (4.7) as

$$\mathbf{G}_0[\kappa_0]\{\boldsymbol{\gamma}_{\text{tot}}^0 \mathbf{E}_{\text{inc}}\} = \begin{cases} -\mathbf{E}_{\text{inc}} & \text{on } \Omega_* = \mathbb{R}^3 \setminus \overline{\Omega}_0, \\ \mathbf{0} & \text{on } \Omega_0. \end{cases} \quad (4.9)$$

Using this intermediate result, we can now simplify the right hand side of (4.5) to

$$\begin{aligned} (\mathbf{Id}_\kappa - \mathbf{M}[\kappa]) \boldsymbol{\epsilon}_{\text{inc},0} &= \mathbf{Id}_\kappa \boldsymbol{\epsilon}_{\text{inc},0} - \mathbf{Id}_{\kappa_0} \boldsymbol{\gamma}_{\text{tot}}^\Sigma \mathbf{G}_0[\kappa_0]\{\boldsymbol{\gamma}_{\text{tot}}^0 \mathbf{E}_{\text{inc}}\} \\ &\stackrel{(*)}{=} \mathbf{Id}_\kappa \boldsymbol{\epsilon}_{\text{inc},0} - \mathbf{Id}_{\kappa_0} (0, -\boldsymbol{\gamma}_{\text{tot}}^1 \mathbf{E}_{\text{inc}}, \dots, -\boldsymbol{\gamma}_{\text{tot}}^L \mathbf{E}_{\text{inc}}) \\ &= \mathbf{Id}_{\kappa_0} \boldsymbol{\gamma}_{\text{tot}}^\Sigma \mathbf{E}_{\text{inc}}, \end{aligned}$$

where $\boldsymbol{\epsilon}_{\text{inc},0} = (\boldsymbol{\gamma}_{\text{tot}}^0 \mathbf{E}_{\text{inc}}, \mathbf{0}, \dots, \mathbf{0})$ and for (*) we applied (4.9) together with $\Omega_i \subset \Omega_*$ for all $i \in \{1, \dots, L\}$. Hence, a simplified version of (4.5) reads

$$(\mathbf{Id}_\kappa - \mathbf{M}[\kappa]) \boldsymbol{\gamma}_{\text{tot}}^\Sigma \mathbf{E} = \mathbf{Id}_{\kappa_0} \boldsymbol{\gamma}_{\text{tot}}^\Sigma \mathbf{E}_{\text{inc}}. \quad (4.10)$$

We choose the skeleton trace $\boldsymbol{\epsilon} = \boldsymbol{\gamma}_{\text{tot}}^\Sigma \mathbf{E} \in \mathcal{ST}(\Sigma)$ of the total field as unknown, insert (4.10) into the bilinear form $\langle\langle \cdot, \cdot \rangle\rangle$ from (3.2) and test with $\mathbf{v} \in \mathcal{MT}(\Sigma)$. This yields the following BIE in variational form ⁴:

Formulation 4.1 *Seek $\boldsymbol{\epsilon} \in \mathcal{ST}(\Sigma)$ such that*

$$\langle\langle (\mathbf{Id}_\kappa - \mathbf{M}) \boldsymbol{\epsilon}, \mathbf{v} \rangle\rangle = \langle\langle \mathbf{Id}_{\kappa_0} \boldsymbol{\epsilon}_{\text{inc}}, \mathbf{v} \rangle\rangle, \quad \forall \mathbf{v} \in \mathcal{MT}(\Sigma), \quad (4.11)$$

where $\boldsymbol{\epsilon}_{\text{inc}} := \boldsymbol{\gamma}_{\text{tot}}^\Sigma \mathbf{E}_{\text{inc}}$.

The next lemma paves the way for a regularized version of Formulation 4.1.

Lemma 4.1 (Regularization) *For all $\kappa, \alpha > 0$ holds⁴*

$$\mathbf{M}[\kappa, \alpha]\{\mathbf{u}\} = \mathbf{0} \quad \forall \mathbf{u} \in \mathcal{ST}(\Sigma). \quad (4.12)$$

⁴ See Remark 4.2 for notation policies.

The proof starts with the key observation that for arguments $\mathbf{u} \in \mathcal{ST}(\Sigma)$ and identical scaling parameters the multi-potential satisfies the transmission conditions (1.2), because all jumps across interfaces cancel. Details of the proof can be found after [13, Lemma 4.1], see also [36, Lemma 6.3.11]. In the end of Section 4.4, we will see that the choice of $\kappa > 0$ does not actually matter.

Using Lemma 4.1, we can *add zero* to (4.11) in the form of

$$\mathbf{M}[\kappa](\mathbf{u}) = \begin{pmatrix} \gamma_{el}^\Sigma \mathbf{M}[\kappa, \kappa](\mathbf{u}) \\ \gamma_m^\Sigma \mathbf{M}[\kappa, 1](\mathbf{u}) \end{pmatrix} = \mathbf{0}, \quad \mathbf{u} \in \mathcal{ST}(\Sigma), \quad \kappa > 0.$$

This gives us a *regularized formulation*.

Formulation 4.2 (Regularized Second-Kind Formulation in Energy Trace Spaces)

For some fixed $\kappa > 0$ seek $\mathbf{e} \in \mathcal{ST}(\Sigma)$ such that

$$\langle\langle (\mathbf{Id}_\kappa - (\mathbf{M} - \mathbf{M}[\kappa])) \mathbf{e}, \mathbf{v} \rangle\rangle = \langle\langle \mathbf{Id}_{\kappa_0} \mathbf{e}_{\text{inc}}, \mathbf{v} \rangle\rangle, \quad \forall \mathbf{v} \in \mathcal{MT}(\Sigma).$$

We now examine the difference operator of Formulation 4.2 more closely in order to justify the attribute “regularized”. For $\mathbf{u} = (\mathbf{u}_0, \dots, \mathbf{u}_L) \in \mathcal{ST}(\Sigma)$, $\mathbf{u}_i = (\mathbf{u}_i, \boldsymbol{\nu}_i) \in \mathcal{T}(\partial\Omega_i)$, mainly using definitions, we find

$$\begin{aligned} & (\mathbf{M} - \mathbf{M}[\kappa])(\mathbf{u}) \\ &= \begin{pmatrix} \gamma_{el}^\Sigma \sum_{i=0}^L (\kappa_i^2 \mathbf{G}_i[\kappa_i] - \kappa^2 \mathbf{G}_i[\kappa])(\mathbf{u}_i) \\ \gamma_m^\Sigma \sum_{i=0}^L (\mathbf{G}_i[\kappa_i] - \mathbf{G}_i[\kappa])(\mathbf{u}_i) \end{pmatrix} \\ &= \begin{pmatrix} \gamma_{el}^j \left\{ \sum_{i=0}^L (-\kappa_i^2 \mathbf{D}_i[\kappa_i] + \kappa^2 \mathbf{D}_i[\kappa])(\mathbf{u}_i) + (\kappa_i^2 \mathbf{V}_i[\kappa_i] - \kappa^2 \mathbf{V}_i[\kappa])(\boldsymbol{\nu}_i) \right. \\ \quad \left. + \mathbf{grad}(\mathbb{V}_i[\kappa_i] - \mathbb{V}_i[\kappa])(\text{div}_\Gamma \boldsymbol{\nu}_i) \right\} \\ \gamma_m^j \left\{ \sum_{i=0}^L (-\mathbf{D}_i[\kappa_i] + \mathbf{D}_i[\kappa])(\mathbf{u}_i) + (\mathbf{V}_i[\kappa_i] - \mathbf{V}_i[\kappa])(\boldsymbol{\nu}_i) \right\} \end{pmatrix}_{j=0}^L \end{aligned}$$

$$\begin{aligned}
&= \left(\sum_{i=0}^L \left\{ \begin{aligned} &\gamma_{el}^j (-\kappa_i^2 \mathbf{D}_i[\kappa_i] + \kappa^2 \mathbf{D}_i[\kappa])(\mathbf{u}_i) \\ &+ \gamma_{el}^j (\kappa_i^2 \mathbf{V}_i[\kappa_i] - \kappa^2 \mathbf{V}_i[\kappa])(\boldsymbol{\nu}_i) \\ &+ \gamma_{el}^j \mathbf{grad}(\nabla_i[\kappa_i] - \nabla_i[\kappa])(\operatorname{div}_\Gamma \boldsymbol{\nu}_i) \end{aligned} \right\} \right)_{j=0}^L \\
&= \left(\sum_{i=0}^L \left\{ \begin{aligned} &-\gamma_\times^j \mathbf{grad}(\nabla_i[\kappa_i] - \nabla_i[\kappa])(\operatorname{curl}_\Gamma \mathbf{u}_i) \\ &+ \gamma_\times^j (\kappa_i^2 \mathbf{V}_i[\kappa_i] - \kappa^2 \mathbf{V}_i[\kappa])(\mathbf{u}_i \times \mathbf{n}_i) \\ &+ \gamma_\times^j \mathbf{curl}(\nabla_i[\kappa_i] - \nabla_i[\kappa])(\boldsymbol{\nu}_i) \end{aligned} \right\} \right)_{j=0}^L, \\
&= \left(\sum_{i=0}^L \gamma_{\mathbf{t}}^j (\delta \mathbf{D}_i(\mathbf{u}_i) + \delta \mathbf{V}_i(\boldsymbol{\nu}_i) + \delta \mathbf{W}_i(\boldsymbol{\nu}_i)) \right)_{j=0}^L \\
&= \left(\sum_{i=0}^L \gamma_\times^j (-\delta \mathbf{W}_i(\mathbf{u}_i \times \mathbf{n}_i) + \delta \mathbf{V}_i(\mathbf{u}_i \times \mathbf{n}_i) + \delta \mathbf{C}_i(\boldsymbol{\nu}_i)) \right)_{j=0}^L,
\end{aligned} \tag{4.13}$$

where we used the following abbreviations for “difference potentials”:

$$\begin{aligned}
\delta \mathbf{D}_i(\mathbf{u}_i) &:= (-\kappa_i^2 \mathbf{D}_i[\kappa_i] + \kappa^2 \mathbf{D}_i[\kappa])(\mathbf{u}_i), \\
\delta \mathbf{V}_i(\boldsymbol{\nu}_i) &:= (\kappa_i^2 \mathbf{V}_i[\kappa_i] - \kappa^2 \mathbf{V}_i[\kappa])(\boldsymbol{\nu}_i), & \mathbf{u}_i \in \mathcal{T}_{el}(\partial\Omega_i), \\
\delta \mathbf{W}_i(\boldsymbol{\nu}_i) &:= \mathbf{grad}(\nabla_i[\kappa_i] - \nabla_i[\kappa])(\operatorname{div}_\Gamma \boldsymbol{\nu}_i), & \boldsymbol{\nu}_i \in \mathcal{T}_m(\partial\Omega_i), \\
\delta \mathbf{C}_i(\boldsymbol{\nu}_i) &:= \mathbf{curl}(\nabla_i[\kappa_i] - \nabla_i[\kappa])(\boldsymbol{\nu}_i). & i \in \{0, \dots, L\}.
\end{aligned} \tag{4.14}$$

The color code has been borrowed from (4.2) to underscore similarities of (4.2) and (4.13). The reader is encouraged to verify that Formulation 4.2 boils down to (4.2) for $L = 1$ and $\kappa = \kappa_0$. Again, in (4.13), we have ended up with differences of boundary integral operators which reward us with the benefits of a cancellation of some leading singularities of their kernels as in Section 4.1. In particular, Formulation 4.2 remains meaningful in \mathbf{L}_t^2 ; it is genuinely 2nd-kind.

Theorem 4.3 (Continuity of Differenced BIOs in $\mathcal{ML}_t(\Sigma)$) *For any real valued $\kappa > 0$, the linear operator $\mathbf{Id}_\kappa - (\mathbf{M} - \mathbf{M}[\kappa])$ can be extended to a continuous mapping $\mathcal{ML}_t(\Sigma) \rightarrow \mathcal{ML}_t(\Sigma)$.*

The proof of Theorem 4.3 can be found in [36, Proof of Thm. 6.3.13]. The assertion can also be concluded from considerations in Section 4.4 below.

Remark 4.4 (Fredholmness of Index Zero) When trying to generalize the result stated in Remark 4.1 to the multi-domain setting, we face problems at triple points, see [36, Remark 6.3.14]. Hitherto it remains open, whether the boundary integral operator of Formulation 4.2 is Fredholm with index 0. Furthermore, the question of existence and uniqueness of solutions of Formulation 4.2 has no answer yet.

4.3 Second-Kind Single-Trace Formulation in $\mathcal{SL}_t(\Sigma)$

As a consequence of Theorem 4.3, the bilinear form on the left-hand side of Formulation 4.2 remains continuous on $\mathcal{ML}_t(\Sigma) \times \mathcal{ML}_t(\Sigma)$, since the pairing $\langle\langle \cdot, \cdot \rangle\rangle$ extends naturally to \mathbf{L}_t^2 . This leads to the *lifted* version of Formulation 4.2.

Formulation 4.4 Fix $\kappa > 0$ and find $\mathbf{e} \in \mathcal{SL}_t(\Sigma)$ such that

$$\langle\langle (\mathbf{Id}_\kappa - (\mathbf{M} - \mathbf{M}[\kappa])) \mathbf{e}, \mathbf{v} \rangle\rangle = \langle\langle \mathbf{Id}_{\kappa_0} \mathbf{e}_{\text{inc}}, \mathbf{v} \rangle\rangle, \quad \forall \mathbf{v} \in \mathcal{ML}_t(\Sigma).$$

Remark 4.5 Electric or magnetic traces of the solution of (1.1) may fail to belong to $\mathbf{L}_t(\Sigma)$, but they will certainly be contained in some Sobolev space $\mathbf{H}_t^{-\delta}(\Sigma)$ of low-regularity tangential vectorfields from some $0 < \delta < \frac{1}{2}$ [20]. This suggests that we consider Formulation 4.4 in $\mathbf{H}_t^{-\delta}(\partial\Omega_i) \times \mathbf{H}_\times^\delta(\partial\Omega_i)$. Since this does not make any difference algorithmically, we are not going to elaborate on this. In any case, Formulation 4.4 will provide an outer approximation of $\gamma_{\text{tot}}^\Sigma \mathbf{E}$.

There is a glaring mismatch of trial and test space in Formulation 4.4 and Formulation 4.2, respectively. A remedy is suggested by the following consequence of Lemma 3.2 (similar to [12, Proposition 5.1] in the acoustic case).

Theorem 4.5

$$\langle\langle (\mathbf{Id}_\kappa - (\mathbf{M} - \mathbf{M}[\kappa])) \mathbf{u}, \mathbf{v} \rangle\rangle = 0, \quad \forall \mathbf{u} \in \mathcal{SL}_t(\Sigma), \forall \mathbf{v} \in \mathcal{SL}_t(\Sigma),$$

The proof of this theorem runs parallel to the proof of the corresponding result for acoustic scattering, see [36, Thm. 6.3.19] for details.

Theorem 4.5 implies, together with the polarity property from Lemma 3.2, that the variational equation from Formulation 4.4 is trivially satisfied for all test functions $\mathbf{v} \in \mathcal{SL}_t(\Sigma)$. Since $\mathcal{SL}_t(\Sigma)$ is a closed subspace of $\mathcal{ML}_t(\Sigma)$, it is sufficient to test with elements in *any* complement space $\mathcal{SL}_t^c(\Sigma)$ of $\mathcal{SL}_t(\Sigma)$ in $\mathcal{ML}_t(\Sigma)$. For the sake of easy implementation we choose $\mathcal{SL}_t^c(\Sigma) := \mathcal{SL}_t^\perp(\Sigma)$, the \mathbf{L}_t^2 -orthogonal complement space. It has the following simple characterization:

Corollary 4.2 (Orthogonal Complement of \mathbf{L}_t^2 -Single-Trace Space)

The orthogonal complement of the skeleton \mathbf{L}_t^2 -single-trace space is given by

$$\mathcal{SL}_t^\perp(\Sigma) := \left\{ \left(\begin{pmatrix} \mathbf{u}_0 \\ \boldsymbol{\nu}_0 \end{pmatrix}, \dots, \begin{pmatrix} \mathbf{u}_L \\ \boldsymbol{\nu}_L \end{pmatrix} \right) \in \mathcal{ML}_t(\Sigma) \mid \mathbf{u}_j|_{\Gamma_{ij}} = -\mathbf{u}_i|_{\Gamma_{ij}}, \boldsymbol{\nu}_j|_{\Gamma_{ij}} = \boldsymbol{\nu}_i|_{\Gamma_{ij}}, \forall j < i \in \{0, \dots, L\} \right\}.$$

Remark 4.6 (Polarity Complement of Energy Single-Trace Space) Since Theorem 4.5 also holds in $\mathcal{MT}(\Sigma)$, in Formulation 4.2 it would be possible to test with elements in *any* complement space $\mathcal{ST}^c(\Sigma)$ of $\mathcal{ST}(\Sigma) \subset \mathcal{MT}(\Sigma)$.

A polarity-complement using the polarity property from Lemma 3.1 seems to be the best choice. But there is no simple representation like the one provided by Corollary 4.2 for the orthogonal complement space $\mathcal{S}\mathcal{L}_t^\perp(\Sigma)$ of $\mathcal{S}\mathcal{L}_t(\Sigma)$. The reason for the lack of such an explicit representation is that restriction to interfaces is in general not well-defined in $\mathcal{MT}(\Sigma)$. Thus Corollary 4.2 reveals a crucial advantage of the \mathbf{L}_t^2 -setting.

Replacing the test space from Formulation 4.4 by the \mathbf{L}_t^2 -orthogonal complement space, we obtain the following formulation.

Formulation 4.6 For $\kappa > 0$ find $\mathbf{e} \in \mathcal{S}\mathcal{L}_t(\Sigma)$ such that

$$\langle\langle (\mathbf{Id}_\kappa - (\mathbf{M} - \mathbf{M}[\kappa])) \mathbf{e}, \mathbf{v} \rangle\rangle = \langle\langle \mathbf{Id}_{\kappa_0} \mathbf{e}_{\text{inc}}, \mathbf{v} \rangle\rangle \quad \forall \mathbf{v} \in \mathcal{S}\mathcal{L}_t^\perp(\Sigma).$$

4.3.1 Second-Kind Formulation in $\mathcal{L}_t^2(\Sigma)$

The definitions of the skeleton spaces $\mathcal{S}\mathcal{L}_t(\Sigma)$ and $\mathcal{S}\mathcal{L}_t^\perp(\Sigma)$ suggest an identification of the spaces with the so-called *interface based \mathbf{L}_t^2 -skeleton space*

$$\mathcal{L}_t^2(\Sigma) := \times_{j < i} (\mathbf{L}_t^2(\Gamma_{ij}) \times \mathbf{L}_t^2(\Gamma_{ij})) \cong \mathbf{L}_t^2(\Sigma) \times \mathbf{L}_t^2(\Sigma). \quad (4.15)$$

The identification \cong is provided by the restriction of tangential vectorfields to interfaces, which is well defined in $\mathbf{L}_t^2(\Sigma)$, and an additional reordering. Definition 3.4 immediately provides the isomorphism $\mathbf{J} : \mathcal{L}_t^2(\Sigma) \rightarrow \mathcal{S}\mathcal{L}_t(\Sigma)$,

$$\mathbf{J} \left((\mathbf{u}_{ij})_{j < i} \right) := \left(\begin{pmatrix} \mathbf{u}_0 \\ \boldsymbol{\nu}_0 \end{pmatrix}, \dots, \begin{pmatrix} \mathbf{u}_L \\ \boldsymbol{\nu}_L \end{pmatrix} \right), \quad \begin{array}{l} \mathbf{u}_i|_{\Gamma_{ij}} := \mathbf{u}_{ij}, \quad \mathbf{u}_j|_{\Gamma_{ij}} := \mathbf{u}_{ij}, \\ \boldsymbol{\nu}_i|_{\Gamma_{ij}} := \boldsymbol{\nu}_{ij}, \quad \boldsymbol{\nu}_j|_{\Gamma_{ij}} := -\boldsymbol{\nu}_{ij}. \end{array} \quad (4.16)$$

for $i, j \in \{0, \dots, L\}$. We also introduce an isomorphism $\mathbf{J}_\perp : \mathcal{L}_t^2(\Sigma) \rightarrow \mathcal{S}\mathcal{L}_t^\perp(\Sigma)$ that identifies elements in $\mathcal{S}\mathcal{L}_t^\perp(\Sigma)$ with elements in $\mathcal{L}_t^2(\Sigma)$ by

$$\mathbf{J}_\perp \left((\mathbf{u}_{ij})_{j < i} \right) := \left(\begin{pmatrix} \mathbf{u}_0 \\ \boldsymbol{\nu}_0 \end{pmatrix}, \dots, \begin{pmatrix} \mathbf{u}_L \\ \boldsymbol{\nu}_L \end{pmatrix} \right), \quad \begin{array}{l} \mathbf{u}_i|_{\Gamma_{ij}} := -\boldsymbol{\nu}_{ij}, \quad \mathbf{u}_j|_{\Gamma_{ij}} := \boldsymbol{\nu}_{ij}, \\ \boldsymbol{\nu}_i|_{\Gamma_{ij}} := \mathbf{u}_{ij}, \quad \boldsymbol{\nu}_j|_{\Gamma_{ij}} := \mathbf{u}_{ij}. \end{array}$$

Moreover, it is immediate that

$$\langle\langle \mathbf{J}\mathbf{u}, \mathbf{J}_\perp \mathbf{v} \rangle\rangle = 2 \llbracket \mathbf{u}, \bar{\mathbf{v}} \rrbracket_{\mathcal{L}_t^2(\Sigma)}, \quad \mathbf{u}, \mathbf{v} \in \mathcal{L}_t^2(\Sigma), \quad (4.17)$$

where $\llbracket \mathbf{u}, \bar{\mathbf{v}} \rrbracket_{\mathcal{L}_t^2(\Sigma)}$ refers to the inner product of $\mathcal{L}_t^2(\Sigma)$ which for $\mathbf{u} = (\mathbf{u}_{ij}, \boldsymbol{\nu}_{ij})_{j < i}$, $\mathbf{v} = (\mathbf{v}_{ij}, \boldsymbol{\varphi}_{ij})_{j < i} \in \mathcal{L}_t^2(\Sigma)$ is given by

$$\llbracket \mathbf{u}, \mathbf{v} \rrbracket_{\mathcal{L}_t^2(\Sigma)} := \sum_{j < i} \left([\mathbf{u}_{ij}, \mathbf{v}_{ij}]_{\Gamma_{ij}} + [\boldsymbol{\nu}_{ij}, \boldsymbol{\varphi}_{ij}]_{\Gamma_{ij}} \right).$$

For the simple proofs we refer to [36, eq. (3.34), (3.35)ff.].

Using the above isomorphisms, Formulation 4.6 can be rewritten in such a way that the trial and test functions belong to $\mathcal{L}_t^2(\Sigma)$.

Formulation 4.7 (Final Second-Kind Formulation)

Seek $\mathbf{e} \in \mathcal{L}_t^2(\Sigma)$ such that

$$\langle\langle (\mathbf{Id}_\kappa - (\mathbf{M} - \mathbf{M}[\kappa])) \mathbf{J}\mathbf{e}, \mathbf{J}_\perp \mathbf{v} \rangle\rangle = \langle\langle \mathbf{Id}_{\kappa_0} \mathbf{e}_{\text{inc}}, \mathbf{J}_\perp \mathbf{v} \rangle\rangle \quad \forall \mathbf{v} \in \mathcal{L}_t^2(\Sigma).$$

Finally we have found a formulation whose Galerkin discretization is straightforward, see Section 5 below.

Remark 4.7 Theorem 4.3 implies only that the operator $\mathbf{Id}_\kappa - (\mathbf{M} - \mathbf{M}[\kappa])$ is continuous. We pointed out that a proof for Fredholmness of index zero is known in the case of $L = 1$, while it is not clear how to generalize the proof to the multi-domain setting $L > 1$. This means that apart from the question of uniqueness of solutions of Formulation 4.7, we cannot guarantee that the operator on the left hand side of Formulation 4.7 is Fredholm of index zero. Thus, well-posedness of the above formulation remains an open problem. Nevertheless, the numerical results provided in Section 6 are promising.

4.4 Interface Based Boundary Integral Equations

Assembly of boundary element Galerkin matrices relies on explicit integral representations of the boundary integral operators occurring in (4.13). Thus, we study the difference potentials from (4.14) for arguments in $\mathcal{L}_t^2(\partial\Omega_i)$.

- By simple calculations we find [9, Eq. (35)] for $\mathbf{x} \notin \partial\Omega_i$

$$\delta\mathbb{D}_i(\mathbf{u}_i)(\mathbf{x}) = \int_{\partial\Omega_i} (-\kappa_i^2 \mathbf{K}_{D,i}[\kappa_i](\mathbf{x}, \mathbf{y}) + \kappa^2 \mathbf{K}_{D,i}[\kappa](\mathbf{x}, \mathbf{y})) \mathbf{u}_i(\mathbf{y}) \, dS(\mathbf{y}),$$

with Cauchy-singular kernel matrices ($\mathbf{x} \notin \partial\Omega_i, \mathbf{y} \in \partial\Omega_i$)

$$\begin{aligned} \mathbf{K}_{D,i}[\kappa](\mathbf{x}, \mathbf{y}) &= \mathbf{n}_i(\mathbf{y}) \mathbf{grad}_x(\Phi_\kappa(\|\mathbf{x} - \mathbf{y}\|))^\top + \\ &\quad (\mathbf{grad}_y(\Phi_\kappa(\|\mathbf{x} - \mathbf{y}\|)) \cdot \mathbf{n}_i(\mathbf{y})) \mathbf{I}_3 \quad \in \mathbb{C}^{3,3}, \end{aligned}$$

behaving like $\|\mathbf{K}_{D,i}[\kappa](\mathbf{x}, \mathbf{y})\| \sim \|\mathbf{x} - \mathbf{y}\|^{-2}$ for $\mathbf{y} \rightarrow \mathbf{x}$.

- Immediately we get the weakly singular integral expression ($\mathbf{x} \in \mathbb{R}^3$)

$$\delta\mathbb{V}_i(\boldsymbol{\nu}_i)(\mathbf{x}) = \int_{\partial\Omega_i} (\kappa_i^2 \Phi_{\kappa_i}(\|\mathbf{x} - \mathbf{y}\|) - \kappa^2 \Phi_\kappa(\|\mathbf{x} - \mathbf{y}\|)) \boldsymbol{\nu}_i(\mathbf{y}) \, dS(\mathbf{y}).$$

- To manipulate $\delta\mathbb{W}_i$ we introduce the *entire* function $\delta\Phi_i(\xi) := (\Phi_{\kappa_i} - \Phi_\kappa)(\xi)$, $\xi \in \mathbb{R}$, and apply integration by parts on $\partial\Omega_i$ and differentiation under the integral ($\mathbf{x} \in \mathbb{R}^3$):

$$\delta\mathbb{W}_i(\boldsymbol{\nu}_i)(\mathbf{x})$$

$$\begin{aligned}
&= \mathbf{grad}_x \int_{\partial\Omega_i} \delta\Phi_i(\|\mathbf{x} - \mathbf{y}\|) (\operatorname{div}_\Gamma \boldsymbol{\nu}_i)(\mathbf{y}) \, dS(\mathbf{y}) \\
&= - \mathbf{grad}_x \int_{\partial\Omega_i} (\mathbf{grad}_y \delta\Phi_i(\|\mathbf{x} - \mathbf{y}\|)) \cdot \boldsymbol{\nu}_i(\mathbf{y}) \, dS(\mathbf{y}) \\
&= \int_{\partial\Omega_i} \left(\frac{\partial^2 \delta\Phi_i}{\partial\xi^2}(\|\mathbf{x} - \mathbf{y}\|) \frac{(\mathbf{x} - \mathbf{y})(\mathbf{x} - \mathbf{y})^\top}{\|\mathbf{x} - \mathbf{y}\|^2} \right. \\
&\quad \left. + \frac{\partial \delta\Phi_i}{\partial\xi}(\|\mathbf{x} - \mathbf{y}\|) \left(\frac{\mathbf{I}_3}{\|\mathbf{x} - \mathbf{y}\|} - \frac{(\mathbf{x} - \mathbf{y})(\mathbf{x} - \mathbf{y})^\top}{\|\mathbf{x} - \mathbf{y}\|^3} \right) \right) \boldsymbol{\nu}_i(\mathbf{y}) \, dS(\mathbf{y}) \\
&= \int_{\partial\Omega_i} (\mathbf{K}_W[\kappa_i](\mathbf{x} - \mathbf{y}) - \mathbf{K}_W[\kappa](\mathbf{x} - \mathbf{y})) \boldsymbol{\nu}_i(\mathbf{y}) \, dS(\mathbf{y}), \quad (4.18)
\end{aligned}$$

where $\mathbf{K}_W[\kappa](\mathbf{x}) \in (C^\infty(\mathbb{R}^3 \setminus \{\mathbf{0}\}))^{3,3}$ is a *weakly singular* integral kernel matrix.

– Even more straightforwardly, we obtain the representation ($\mathbf{x} \in \mathbb{R}^3$)

$$\begin{aligned}
\delta\mathbf{C}_i(\boldsymbol{\nu}_i)(\mathbf{x}) &= \int_{\partial\Omega_i} -\frac{\partial \delta\Phi_i}{\partial\xi}(\|\mathbf{x} - \mathbf{y}\|) \frac{\mathbf{y} - \mathbf{x}}{\|\mathbf{x} - \mathbf{y}\|} \times \boldsymbol{\nu}_i(\mathbf{y}) \, dS(\mathbf{y}) \\
&= \int_{\partial\Omega_i} (\mathbf{K}_C[\kappa_i](\mathbf{x} - \mathbf{y}) - \mathbf{K}_C[\kappa](\mathbf{x} - \mathbf{y})) \boldsymbol{\nu}_i(\mathbf{y}) \, dS(\mathbf{y}), \quad (4.19)
\end{aligned}$$

with a bounded kernel matrix $\mathbf{K}_{C,\kappa}(\mathbf{x}) \in (C^\infty(\mathbb{R}^3 \setminus \{\mathbf{0}\}))^{3,3} \cap (L^\infty(\mathbb{R}^3))^{3,3}$.

A more detailed presentation of these kernels including series expansions for $\mathbf{x} \approx \mathbf{y}$ can be found in [36, Appendix A]. In fact, the above manipulations confirm Theorem 4.5, because no hypersingular kernels occur so that boundary integral operators spawned by applying tangential traces to difference potentials can take arguments in $\mathbf{L}_t^2(\partial\Omega_i)$.

Remark 4.8 In Formula (4.18) all derivatives have been shifted off the argument function $\boldsymbol{\nu}_i$. This was made possible by our regularization, which introduced more regular differences of singular kernels that allow differentiation. Hence, the regularity of $\operatorname{div}_\Gamma(\mathbf{n}_i \times \mathbf{u})$ and $\operatorname{div}_\Gamma \boldsymbol{\nu}$ becomes irrelevant. As regards boundary element Galerkin discretization, $\operatorname{div}_\Gamma$ -conformity of the trial and test spaces is no longer required!

Thanks to the regularity of their kernels the difference potentials can be considered on parts of a subdomain boundary, in particular on interfaces Γ_{ij} . We pick $\mathbf{u} = (\mathbf{u}_{ij})_{j < i} \in \mathcal{L}_t^2(\Sigma)$, $\mathbf{u}_{ij} = \begin{pmatrix} \mathbf{u}_{ij} \\ \boldsymbol{\nu}_{ij} \end{pmatrix} \in \mathbf{L}_t^2(\Gamma_{ij}) \times \mathbf{L}_t^2(\Gamma_{ij})$, $i, j \in \{0, \dots, L\}$ and, by switching to summation over interfaces, convert (4.13) into

$$(\mathbf{M} - \mathbf{M}[\kappa])\mathbf{J}\mathbf{u} =$$

$$\left(\begin{array}{l} \gamma_{\mathbf{t}}^n \sum_{j < i} \left(\begin{array}{l} \delta \mathbb{D}_i(\mathbf{u}_{ij}) + \delta \mathbb{V}_i(\boldsymbol{\nu}_{ij}) + \delta \mathbb{W}_i(\boldsymbol{\nu}_{ij}) \\ + \delta \mathbb{D}_j(\mathbf{u}_{ij}) - \delta \mathbb{V}_j(\boldsymbol{\nu}_{ij}) - \delta \mathbb{W}_j(\boldsymbol{\nu}_{ij}) \end{array} \right) \\ \gamma_{\times}^n \sum_{j < i} \left(\begin{array}{l} -\delta \mathbb{W}_i(\mathbf{u}_{ij} \times \mathbf{n}_i) + \delta \mathbb{V}_i(\mathbf{u}_{ij} \times \mathbf{n}_i) + \delta \mathbb{C}_i(\boldsymbol{\nu}_{ij}) \\ -\delta \mathbb{W}_j(\mathbf{u}_{ij} \times \mathbf{n}_j) + \delta \mathbb{V}_j(\mathbf{u}_{ij} \times \mathbf{n}_j) - \delta \mathbb{C}_j(\boldsymbol{\nu}_{ij}) \end{array} \right) \end{array} \right)_{n=0}^L .$$

The signs of the difference potential contributions are derived from (4.16). We point out that an extension by zero of \mathbf{u}_{ij} and $\boldsymbol{\nu}_{ij}$ to both $\partial\Omega_i$ and $\partial\Omega_j$ has been tacitly assumed here.

Next, we exploit cancellation due to opposite orientations of the normals $\mathbf{n}_i = -\mathbf{n}_j$ on Γ_{ij} . We make the surprising discovery that all contributions due to the regularizing operator $\mathbf{M}[\kappa]$ can be dropped: Eventually, the choice of $\kappa > 0$ does not matter!

$$\begin{aligned} \delta \mathbb{D}_{ij}(\mathbf{u}_{ij}) &:= \delta \mathbb{D}_i(\mathbf{u}_{ij}) + \delta \mathbb{D}_j(\mathbf{u}_{ij}) \\ &= -\kappa_i^2 \mathbb{D}_i[\kappa_i](\mathbf{u}_{ij}) + \kappa^2 \mathbb{D}_i[\kappa](\mathbf{u}_{ij}) - \kappa_j^2 \mathbb{D}_j[\kappa_j](\mathbf{u}_{ij}) + \kappa^2 \mathbb{D}_j[\kappa](\mathbf{u}_{ij}) \\ &= (-\kappa_i^2 \mathbb{D}_i[\kappa_i] - \kappa_j^2 \mathbb{D}_j[\kappa_j])(\mathbf{u}_{ij}) \\ &= \int_{\Gamma_{ij}} \underbrace{(-\kappa_i^2 \mathbf{K}_{D,i}[\kappa_i](\cdot, \mathbf{y}) + \kappa_j^2 \mathbf{K}_{D,i}[\kappa_j](\cdot, \mathbf{y}))}_{=: \delta \mathbf{K}_{D,ij}(\cdot, \mathbf{y})} \mathbf{u}_{ij}(\mathbf{y}) \, dS(\mathbf{y}) , \end{aligned}$$

$$\begin{aligned} \delta \mathbb{V}_{ij}(\boldsymbol{\nu}_{ij}) &:= \delta \mathbb{V}_i(\boldsymbol{\nu}_{ij}) - \delta \mathbb{V}_j(\boldsymbol{\nu}_{ij}) \\ &= \kappa_i^2 \mathbb{V}_i[\kappa_i](\boldsymbol{\nu}_{ij}) - \kappa^2 \mathbb{V}_i[\kappa](\boldsymbol{\nu}_{ij}) - \kappa_j^2 \mathbb{V}_j[\kappa_j](\boldsymbol{\nu}_{ij}) + \kappa^2 \mathbb{V}_j[\kappa](\boldsymbol{\nu}_{ij}) \\ &= \kappa_i^2 \mathbb{V}_i[\kappa_i](\boldsymbol{\nu}_{ij}) - \kappa_j^2 \mathbb{V}_j[\kappa_j](\boldsymbol{\nu}_{ij}) \\ &= \int_{\Gamma_{ij}} \underbrace{(\kappa_i^2 \Phi_{\kappa_i}(\|\cdot - \mathbf{y}\|) - \kappa_j^2 \Phi_{\kappa_j}(\|\cdot - \mathbf{y}\|))}_{=: \delta \mathbf{K}_{V,ij}(\cdot, \mathbf{y})} \boldsymbol{\nu}_{ij}(\mathbf{y}) \, dS(\mathbf{y}) , \end{aligned}$$

$$\begin{aligned} \delta \mathbb{W}_{ij}(\boldsymbol{\nu}_{ij}) &:= \delta \mathbb{W}_i(\boldsymbol{\nu}_{ij}) - \delta \mathbb{W}_j(\boldsymbol{\nu}_{ij}) \\ &= \int_{\Gamma_{ij}} \underbrace{(\mathbf{K}_W[\kappa_i](\cdot - \mathbf{y}) - \mathbf{K}_W[\kappa_j](\cdot - \mathbf{y}))}_{=: \delta \mathbf{K}_{W,ij}(\cdot, \mathbf{y})} \boldsymbol{\nu}_{ij}(\mathbf{y}) \, dS(\mathbf{y}) , \end{aligned}$$

$$\begin{aligned} \delta \mathbb{C}_{ij}(\boldsymbol{\nu}_{ij}) &:= \delta \mathbb{C}_i(\boldsymbol{\nu}_{ij}) - \delta \mathbb{C}_j(\boldsymbol{\nu}_{ij}) \\ &= \int_{\Gamma_{ij}} \underbrace{(\mathbf{K}_C[\kappa_i](\cdot - \mathbf{y}) - \mathbf{K}_C[\kappa_j](\cdot - \mathbf{y}))}_{=: \delta \mathbf{K}_{C,ij}(\cdot, \mathbf{y})} \boldsymbol{\nu}_{ij}(\mathbf{y}) \, dS(\mathbf{y}) . \end{aligned}$$

Note that among these difference potentials $\delta \mathbb{D}_{ij}(\mathbf{u}_{ij})$ is the only one that may be discontinuous across Γ_{ij} , because from the jump relations (2.9) we conclude ($i, j, m \in \{0, \dots, L\}, j < i$)

$$\gamma_{el}^i \delta \mathbb{D}_{ij}(\mathbf{u}_{ij}) = \frac{1}{2}(\kappa_i^2 - \kappa_j^2) \mathbf{u}_{ij} + \delta \mathbb{D}_{ij}^i(\mathbf{u}_{ij}) \quad \text{on } \partial\Omega_i , \quad (4.20)$$

$$\gamma_{el}^j \delta \mathbb{D}_{ij}(\mathbf{u}_{ij}) = \frac{1}{2}(\kappa_j^2 - \kappa_i^2) \mathbf{u}_{ij} + \delta \mathbb{D}_{ij}^j(\mathbf{u}_{ij}) \quad \text{on } \partial\Omega_j ,$$

$$\gamma_{el}^m \delta \mathbb{D}_{ij}(\mathbf{u}_{ij}) = \delta \mathbb{D}_{ij}^m(\mathbf{u}_{ij}) \quad \text{on } \partial\Omega_m , m \notin \{i, j\} , \quad (4.21)$$

where the boundary integral operators $\delta\mathbf{D}_{ij}^m : \mathbf{L}_t^2(\Gamma_{ij}) \rightarrow \mathbf{L}_t^2(\partial\Omega_m)$ are defined as

$$(\delta\mathbf{D}_{ij}^m \mathbf{u}_{ij})(\mathbf{x}) := \int_{\Gamma_{ij}} \pi_{\mathbf{t},m}(\mathbf{x}) \delta\mathbf{K}_{D,ij}(\mathbf{x}, \mathbf{y}) \mathbf{u}_{ij}(\mathbf{y}) \, dS(\mathbf{y}), \quad \mathbf{x} \in \partial\Omega_m, \quad (4.22)$$

with $\pi_{\mathbf{t},m}(\mathbf{x})$ designating the orthogonal projection onto the tangent plane of $\partial\Omega_m$ in \mathbf{x} . In a similar fashion we introduce the boundary integral operators listed in the following tables along with their kernels

BI-Op.	$\delta\mathbf{D}_{ij}^m$	$\delta\mathbf{V}_{ij}^m$	$\delta\mathbf{W}_{ij}$
kernel	$\pi_{\mathbf{t},m}(\mathbf{x}) \delta\mathbf{K}_{D,ij}(\mathbf{x}, \mathbf{y})$	$\pi_{\mathbf{t},m}(\mathbf{x}) \delta\mathbf{K}_{V,ij}(\mathbf{x}, \mathbf{y})$	$\pi_{\mathbf{t},m}(\mathbf{x}) \delta\mathbf{K}_{W,ij}(\mathbf{x}, \mathbf{y})$
BI-Op.	$\delta\tilde{\mathbf{W}}_{ij}^m$	$\delta\tilde{\mathbf{V}}_{ij}^m$	$\delta\mathbf{C}_{ij}^m$
kernel	$\pi_{\times,m}(\mathbf{x}) \delta\mathbf{K}_{W,ij}(\mathbf{x}, \mathbf{y})$	$\pi_{\times,m}(\mathbf{x}) \delta\mathbf{K}_{V,ij}(\mathbf{x}, \mathbf{y})$	$\pi_{\times,m}(\mathbf{x}) \delta\mathbf{K}_{C,ij}(\mathbf{x}, \mathbf{y})$

Table 4.1: Boundary integral operators and their kernels

where $\pi_{\times,m}(\mathbf{x})$ stands for the action of $-\mathbf{n}_m(\mathbf{x}) \times \pi_{\mathbf{t},m}$. Using these boundary integral operators and the jump relations (4.20) we can recast

$$\begin{aligned}
& (\mathbf{M} - \mathbf{M}[\kappa]) \mathbf{J}\mathbf{u} \\
&= \left(\begin{array}{c} \gamma_{\mathbf{t}}^m \sum_{j<i} (\delta\mathbb{D}_{ij}(\mathbf{u}_{ij}) + \delta\mathbb{V}_{ij}(\boldsymbol{\nu}_{ij}) + \delta\mathbb{W}_{ij}(\boldsymbol{\nu}_{ij})) \\ \gamma_{\times}^m \sum_{j<i} (-\delta\mathbb{W}_{ij}(\mathbf{u}_{ij} \times \mathbf{n}_i) + \delta\mathbb{V}_{ij}(\mathbf{u}_{ij} \times \mathbf{n}_i) + \delta\mathbb{C}_{ij}(\boldsymbol{\nu}_{ij})) \end{array} \right)_{m=0}^L \\
&= \left(\begin{array}{c} \sum_{j=0}^{m-1} \frac{1}{2} (\kappa_m^2 - \kappa_j^2) \mathbf{u}_{mj} + \sum_{i=m+1}^L \frac{1}{2} (\kappa_m^2 - \kappa_i^2) \mathbf{u}_{im} \\ + \sum_{j<i} \delta\mathbf{D}_{ij}^m(\mathbf{u}_{ij}) + \delta\mathbf{V}_{ij}^m(\boldsymbol{\nu}_{ij}) + \delta\mathbf{W}_{ij}^m(\boldsymbol{\nu}_{ij}) \\ \sum_{j<i} -\delta\tilde{\mathbf{W}}_{ij}^m(\mathbf{u}_{ij} \times \mathbf{n}_i) + \delta\tilde{\mathbf{V}}_{ij}^m(\mathbf{u}_{ij} \times \mathbf{n}_i) + \delta\mathbf{C}_{ij}^m(\boldsymbol{\nu}_{ij}) \end{array} \right)_{m=0}^L \quad (4.23)
\end{aligned}$$

This formula can be inserted into the variational equation of Formulation 4.7 using

$$\langle\langle \mathbf{w}, \mathbf{J}_{\perp} \mathbf{v} \rangle\rangle = \sum_{l<k} \int_{\Gamma_{kl}} \mathbf{w}_k \cdot \mathbf{v}_{kl} + \boldsymbol{\omega}_k \cdot \boldsymbol{\phi}_{kl} + \mathbf{w}_l \cdot \mathbf{v}_{kl} - \boldsymbol{\omega}_l \cdot \boldsymbol{\phi}_{kl} \, dS,$$

for $\mathbf{w} = \left((\mathbf{w}_0^L), \dots, (\mathbf{w}_L^L) \right) \in \mathcal{ML}(\Sigma)$ and $\mathbf{v} = \left((\mathbf{v}_{kl}^L), (\boldsymbol{\phi}_{kl}^L) \right)_{l<k} \in \mathcal{L}_t^2(\Sigma)$, which follows from (3.3). This implies an *interface-oriented* way to express the left-hand side of Formulation 4.7:

$$\langle\langle (\mathbf{Id}_{\kappa} - (\mathbf{M} - \mathbf{M}[\kappa])) \mathbf{J}\mathbf{u}, \mathbf{J}_{\perp} \mathbf{v} \rangle\rangle$$

$$\begin{aligned}
&= \sum_{l < k} \int_{\Gamma_{kl}} (\kappa_k^2 + \kappa_l^2) \mathbf{u}_{kl} \cdot \mathbf{v}_{kl} \, dS \\
&\quad + \sum_{l < k} \sum_{j < i} \int_{\Gamma_{kl}} \left((\delta D_{ij}^k + \delta D_{ij}^l)(\mathbf{u}_{ij}) \right. \\
&\quad \quad \quad + (\delta \mathbf{V}_{ij}^k + \delta \mathbf{V}_{ij}^l)(\boldsymbol{\nu}_{ij}) \\
&\quad \quad \quad \left. + (\delta \mathbf{W}_{ij}^k + \delta \mathbf{W}_{ij}^l)(\boldsymbol{\nu}_{ij}) \right) \cdot \mathbf{v}_{kl} \, dS \\
&\quad + \int_{\Gamma_{kl}} \left((-\delta \tilde{\mathbf{W}}_{ij}^k + \delta \tilde{\mathbf{W}}_{ij}^l)(\mathbf{u}_{ij} \times \mathbf{n}_i) \right. \\
&\quad \quad \quad + (\delta \tilde{\mathbf{V}}_{ij}^k - \delta \tilde{\mathbf{V}}_{ij}^l)(\mathbf{u}_{ij} \times \mathbf{n}_i) \\
&\quad \quad \quad \left. + (\delta \mathbf{C}_{ij}^k - \delta \mathbf{C}_{ij}^l)(\boldsymbol{\nu}_{ij}) \right) \cdot \boldsymbol{\phi}_{kl} \, dS \tag{4.24} \\
&= \sum_{l < k} \int_{\Gamma_{kl}} (\kappa_k^2 + \kappa_l^2) \mathbf{u}_{kl} \cdot \mathbf{v}_{kl} \, dS \\
&\quad + 2 \sum_{l < k} \sum_{j < i} \int_{\Gamma_{kl}} \left(\delta D_{ij}^k(\mathbf{u}_{ij}) + \delta \mathbf{V}_{ij}^k(\boldsymbol{\nu}_{ij}) + \delta \mathbf{W}_{ij}^k(\boldsymbol{\nu}_{ij}) \right) \cdot \mathbf{v}_{kl} \, dS \\
&\quad + \int_{\Gamma_{kl}} \left(-\delta \tilde{\mathbf{W}}_{ij}^k(\mathbf{u}_{ij} \times \mathbf{n}_i) + \delta \tilde{\mathbf{V}}_{ij}^k(\mathbf{u}_{ij} \times \mathbf{n}_i) \right. \\
&\quad \quad \quad \left. + \delta \mathbf{C}_{ij}^k(\boldsymbol{\nu}_{ij}) \right) \cdot \boldsymbol{\phi}_{kl} \, dS.
\end{aligned}$$

For Galerkin discretization this is the most appropriate form of Formulation 4.7.

5 Galerkin Discretization

For the Galerkin discretization of the variational problem from Formulation 4.7 it remains to specify finite dimensional boundary element spaces $V_M \subset \mathcal{L}_{\mathbf{t}}^2(\Sigma)$ and sets of basis functions. This is done in the next Section. In Section 5.2, we explicitly state the Galerkin system corresponding to Formulation 4.7 for a simple geometric arrangement with $L = 2$.

5.1 Boundary Element Spaces

We rely on a mesh partition \mathcal{T}_M of Σ , compatible with the interfaces in the sense that the closure of each interface Γ_{ij} is the union of some (closed) cells of \mathcal{T}_M . For each cell τ of \mathcal{T}_M we assume the existence of a polygonal reference cell $\hat{\tau} \subset \mathbb{R}^2$ and a C^1 -diffeomorphism $\Phi_\tau : \hat{\tau} \rightarrow \tau$.

Definition 5.1 (Piecewise polynomial Tangential Vector Fields) For $k \in \mathbb{N}_0$, we define the space of \mathcal{T}_M -piecewise polynomial tangential vector fields of degree $\leq k$ by

$$\mathcal{V}_{\mathcal{T}_M}^k(\Sigma) = \left\{ \mathbf{v} \in L^\infty(\Sigma)^3 \mid \mathbf{v}|_\tau \in \mathbf{F}_{\mathbf{t},\tau}((\mathcal{P}_k(\hat{\tau}))^2), \forall \tau \in \mathcal{T}_M \right\},$$

where $\mathbf{F}_{\mathbf{t},\tau}$ denotes the covariant transformation

$$\begin{aligned}\mathbf{F}_{\mathbf{t},\tau}\{\mathbf{p}\}(\mathbf{x}) &:= \mathbf{D}\Phi_\tau(\widehat{\mathbf{x}})(\mathbf{G}_\tau(\widehat{\mathbf{x}}))^{-1}\mathbf{p}(\widehat{\mathbf{x}}), \\ \mathbf{G}_\tau(\mathbf{x}) &:= (\mathbf{D}\Phi_\tau(\widehat{\mathbf{x}}))^\top \mathbf{D}\Phi_\tau(\widehat{\mathbf{x}}), \quad \widehat{\mathbf{x}} = \Phi_\tau^{-1}(\mathbf{x}), \quad \mathbf{x} \in \tau,\end{aligned}$$

and $\mathcal{P}_k(\widehat{\tau})$ is the space of polynomials of degree $\leq k$ on $\widehat{\tau}$.

Then, as trial and test space for Formulation 4.7 we may choose

$$V_M := \mathcal{V}_{\mathcal{T}_M}^k(\Sigma) \times \mathcal{V}_{\mathcal{T}_M}^k(\Sigma) \subset \mathcal{L}_{\mathbf{t}}^2(\Sigma). \quad (5.1)$$

Now we restrict ourselves to approximation by piecewise constant vector fields, that is, $k = 0$. In this case, writing M for the number of cells of \mathcal{T}_M , we can use the basis $\{\chi_M^i\}_{i \in \{1, \dots, 2M\}}$ of $\mathcal{V}_{\mathcal{T}_M}^0(\Sigma)$, whose elements are given by

$$\begin{aligned}\chi_M^{2(i-1)+1}(\mathbf{x}) &= \begin{cases} \mathbf{F}_{\mathbf{t},\tau_i} \left(\begin{pmatrix} 1 \\ 0 \end{pmatrix} \right) & \mathbf{x} \in \tau_i, \\ \mathbf{0} & \mathbf{x} \notin \tau_i, \end{cases} & \tau_i \in \mathcal{T}_M := \{\tau_1, \dots, \tau_M\}, \\ \chi_M^{2(i-1)+2}(\mathbf{x}) &= \begin{cases} \mathbf{F}_{\mathbf{t},\tau_i} \left(\begin{pmatrix} 0 \\ 1 \end{pmatrix} \right) & \mathbf{x} \in \tau_i, \\ \mathbf{0} & \mathbf{x} \notin \tau_i, \end{cases} & i \in \{1, \dots, M\}.\end{aligned} \quad (5.2)$$

Thus we obtain a basis for $V_M = \mathcal{V}_{\mathcal{T}_M}^0(\Sigma) \times \mathcal{V}_{\mathcal{T}_M}^0(\Sigma)$, namely

$$\mathcal{B}_M := \{b_M^q\}_{q=1}^{\dim V_M} = \left\{ \left(\chi_M^1, 0 \right), \dots, \left(\chi_M^{2M}, 0 \right), \left(0, \chi_M^1 \right), \dots, \left(0, \chi_M^{2M} \right) \right\}. \quad (5.3)$$

5.2 Galerkin Matrices

For the sake of lucidity, we will discuss the linear system of equations arising from the Galerkin discretization of Formulation 4.7 with \mathcal{T}_M -piecewise constant vectorfields ($V_M = \mathcal{V}_{\mathcal{T}_M}^0(\Sigma) \times \mathcal{V}_{\mathcal{T}_M}^0(\Sigma)$) only for special situation of two hemispherical subdomains, see Figure 5.1 for a cross-section. This situation is sufficiently general to convey all key considerations.

We order the cells of \mathcal{T}_M according to their occurrence in the interfaces Γ_{21}, Γ_{20} , and Γ_{10} and use the basis (5.3), designating the basis functions by b_M^q , $q = 1, \dots, 2M$. We can represent an element $\mathbf{e}_M \in V_M \subset \mathcal{L}_{\mathbf{t}}^2(\Sigma)$ as $\mathbf{e}_M = \sum_{q=1}^{\dim V_M} e_{q,M} b_M^q$ with a coefficient vector $\vec{\mathbf{e}}_M \in \mathbb{C}^{2M}$. The interface-aware ordering of mesh cells and the corresponding ordering of basis functions, induces a partitioning of the coefficient vector according to

$$\vec{\mathbf{e}}_M = (\vec{\mathbf{e}}_{21,M}, \vec{\mathbf{e}}_{20,M}, \vec{\mathbf{e}}_{10,M}, \vec{\mathbf{\varphi}}_{21,M}, \vec{\mathbf{\varphi}}_{20,M}, \vec{\mathbf{\varphi}}_{10,M}), \quad (5.4)$$

where $\vec{\mathbf{e}}_{ij,M} \in \mathbb{C}^{2M_{ij}}$ is the $2M_{ij}$ -vector of expansion coefficients, $M_{ij} \in \mathbb{N}$ the number of mesh cells $\subset \Gamma_{ij}$, belonging to basis functions supported on Γ_{ij} . We point out that the colors indicate the interface to which sub-vectors are associated. They match the colors in Figure 5.1.

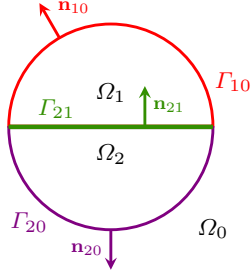


Fig. 5.1: Cross-section of the model geometry ($L = 2$) for studying the implementation of the second-kind formulation.

Inserting the ansatz into Formulation 4.7 and using the the interface-wise representation of its left hand side from (4.24) yields the following linear system of equations:

$$\mathbf{G}_M \mathbf{e}_M = \mathbf{f}_M,$$

with $\mathbf{f}_M \in \mathbb{C}^{2M}$ and the Galerkin matrix $\mathbf{G}_M \in \mathbb{C}^{2M, 2M}$,

$$\mathbf{f}_M := \begin{pmatrix} 2\kappa_0^2 M_{21}^{21} & 0 & 0 & 0 & 0 & 0 \\ 0 & 2\kappa_0^2 M_{20}^{20} & 0 & 0 & 0 & 0 \\ 0 & 0 & 2\kappa_0^2 M_{10}^{10} & 0 & 0 & 0 \\ 0 & 0 & 0 & 2M_{21}^{21} & 0 & 0 \\ 0 & 0 & 0 & 0 & 2M_{20}^{20} & 0 \\ 0 & 0 & 0 & 0 & 0 & 2M_{10}^{10} \end{pmatrix} \begin{pmatrix} \mathbf{e}_{\text{inc}21,M} \\ \mathbf{e}_{\text{inc}20,M} \\ \mathbf{e}_{\text{inc}10,M} \\ \varphi_{\text{inc}21,M} \\ \varphi_{\text{inc}20,M} \\ \varphi_{\text{inc}10,M} \end{pmatrix},$$

where $(\mathbf{e}_{\text{inc}21,M}, \mathbf{e}_{\text{inc}20,M}, \mathbf{e}_{\text{inc}10,M}, \varphi_{\text{inc}21,M}, \varphi_{\text{inc}20,M}, \varphi_{\text{inc}10,M}) \in \mathbb{C}^{2M}$ represents the coefficient vector of the interpolant of $\mathbf{J}^{-1} \mathbf{e}_{\text{inc}} = \mathbf{J}^{-1} \boldsymbol{\gamma}_{\text{tot}}^\Sigma \mathbf{E}_{\text{inc}}$ in V_M and

$$\mathbf{G}_M = \begin{pmatrix} (\kappa_2^2 + \kappa_1^2) M_{21}^{21} & 0 & 0 & 0 & 0 & 0 \\ 0 & (\kappa_2^2 + \kappa_0^2) M_{20}^{20} & 0 & 0 & 0 & 0 \\ 0 & 0 & (\kappa_1^2 + \kappa_0^2) M_{10}^{10} & 0 & 0 & 0 \\ 0 & 0 & 0 & 2M_{21}^{21} & 0 & 0 \\ 0 & 0 & 0 & 0 & 2M_{20}^{20} & 0 \\ 0 & 0 & 0 & 0 & 0 & 2M_{10}^{10} \end{pmatrix} - 2 \begin{pmatrix} \delta D_{21}^{21} & \delta D_{20}^{21} & \delta D_{10}^{21} & \delta V_{21}^{21} + \delta W_{21}^{21} & \delta V_{20}^{21} + \delta W_{20}^{21} & \delta V_{10}^{21} + \delta W_{10}^{21} \\ \delta D_{21}^{20} & \delta D_{20}^{20} & \delta D_{10}^{20} & \delta V_{21}^{20} + \delta W_{21}^{20} & \delta V_{20}^{20} + \delta W_{20}^{20} & \delta V_{10}^{20} + \delta W_{10}^{20} \\ \delta D_{21}^{10} & \delta D_{20}^{10} & \delta D_{10}^{10} & \delta V_{21}^{10} + \delta W_{21}^{10} & \delta V_{20}^{10} + \delta W_{20}^{10} & \delta V_{10}^{10} + \delta W_{10}^{10} \\ \delta \tilde{V}_{21}^{21} + \delta \tilde{W}_{21}^{21} & \delta \tilde{V}_{20}^{21} + \delta \tilde{W}_{20}^{21} & \delta \tilde{V}_{10}^{21} + \delta \tilde{W}_{10}^{21} & \delta C_{21}^{21} & \delta C_{20}^{21} & \delta C_{10}^{21} \\ \delta \tilde{V}_{21}^{20} + \delta \tilde{W}_{21}^{20} & \delta \tilde{V}_{20}^{20} + \delta \tilde{W}_{20}^{20} & \delta \tilde{V}_{10}^{20} + \delta \tilde{W}_{10}^{20} & \delta C_{21}^{20} & \delta C_{20}^{20} & \delta C_{10}^{20} \\ \delta \tilde{V}_{21}^{10} + \delta \tilde{W}_{21}^{10} & \delta \tilde{V}_{20}^{10} + \delta \tilde{W}_{20}^{10} & \delta \tilde{V}_{10}^{10} + \delta \tilde{W}_{10}^{10} & \delta C_{21}^{10} & \delta C_{20}^{10} & \delta C_{10}^{10} \end{pmatrix}.$$

The Galerkin interface mass matrix for Γ_{ij} is given by

$$\mathbf{M}_{ij}^{ij} := \left(\int_{\Gamma_{ij}} \chi_{ij,M}^q \cdot \chi_{ij,M}^s dS \right)_{s,q \in \{1, \dots, 2M_{ij}\}},$$

and the block matrices $\delta\mathbf{D}_{ij}^{kl}$, $\delta\mathbf{V}_{ij}^{kl}$, $\delta\mathbf{W}_{ij}^{kl}$, $\delta\widetilde{\mathbf{V}}_{ij}^{kl}$, $\delta\widetilde{\mathbf{W}}_{ij}^{kl}$, $\delta\mathbf{C}_{ij}^{kl} \in \mathbb{C}^{2M_{kl}, 2M_{ij}}$ have the entries

$$\begin{aligned} (\delta\mathbf{D}_{ij}^{kl})_{s,q} &:= \int_{\Gamma_{kl}} \delta\mathbf{D}_{ij}^k(\chi_{ij,M}^q) \cdot \chi_{kl,M}^s \, dS, & (\delta\mathbf{C}_{ij}^{kl})_{s,q} &:= \int_{\Gamma_{kl}} \delta\mathbf{C}_{ij}^k(\chi_{ij,M}^q) \cdot \chi_{kl,M}^s \, dS, \\ (\delta\mathbf{V}_{ij}^{kl})_{s,q} &:= \int_{\Gamma_{kl}} \delta\mathbf{V}_{ij}^k(\chi_{ij,M}^q) \cdot \chi_{kl,M}^s \, dS, & (\delta\widetilde{\mathbf{V}}_{ij}^{kl})_{s,q} &:= \int_{\Gamma_{kl}} \delta\widetilde{\mathbf{V}}_{ij}^k(\chi_{ij,M}^q \times \mathbf{n}_i) \cdot \chi_{kl,M}^s \, dS, \\ (\delta\mathbf{W}_{ij}^{kl})_{s,q} &:= \int_{\Gamma_{kl}} \delta\mathbf{W}_{ij}^k(\chi_{ij,M}^q) \cdot \chi_{kl,M}^s \, dS, & (\delta\widetilde{\mathbf{W}}_{ij}^{kl})_{s,q} &:= \int_{\Gamma_{kl}} \delta\widetilde{\mathbf{W}}_{ij}^k(\chi_{ij,M}^q \times \mathbf{n}_i) \cdot \chi_{kl,M}^s \, dS. \end{aligned}$$

In each case $s \in \{1, \dots, M_{kl}\}$, $q \in \{1, \dots, M_{ij}\}$, and χ_{mn}^r is the r -th piecewise constant basis function according to (5.2) on the interface Γ_{mn} . The definitions of the involved boundary integral operators can be found in Table 4.1 and (4.22).

6 Numerical Results

In numerical experiments we study the convergence of Galerkin solutions of Formulation 4.7. We also compare their accuracy with that of Galerkin solutions obtained with the the PMCHWT formulation based on *classical low-order curl $_{\Sigma}$ and div $_{\Sigma}$ -conforming edge elements*, also known as *Nédélec and Raviart-Thomas elements*, respectively, see e.g. [36, Form. 6.4.2].

All computations were done by the C++ boundary element software BETL [26], employing the transformation techniques from [35, Chapter 5] to treat singular integrals combined with high order numerical quadrature whose impact is likely to be negligible. Numerically stable formulas for difference kernels were used, see [17, Section 5] or [36, Section 3.5.2]. Computations of Euclidean condition numbers or spectra of matrices were done in MATLAB.

6.1 Model Problems

We discuss four different scattering problems based on the two different geometries depicted in Figure 6.1 and Figure 6.2, respectively.⁵ More numerical experiments can be found in [36, Section 6.6].

Experiment I. We solve the electromagnetic scattering problem with incident plane wave $\mathbf{E}_{\text{inc}}(\mathbf{x}) = \mathbf{p} \exp(i\kappa_0 \mathbf{d} \cdot \mathbf{x})$, $\mathbf{x} \in \mathbb{R}^3$, propagating into direction $\mathbf{d} = (1, 0, 0)^\top$ with polarization $\mathbf{p} = (0, 1, 0)^\top$, impinging on a ball-shaped scattering object $\Omega_* := \mathcal{B}_{0.5}(\mathbf{0})$ of radius $r = 0.5$, centered at the origin. A picture of the geometry is given in Fig. 6.1. The scatterer is split into two hemispheres Ω_1 and Ω_2 and the wave numbers are chosen as $(\kappa_0, \kappa_1, \kappa_2) = (2, 3, 1)$.

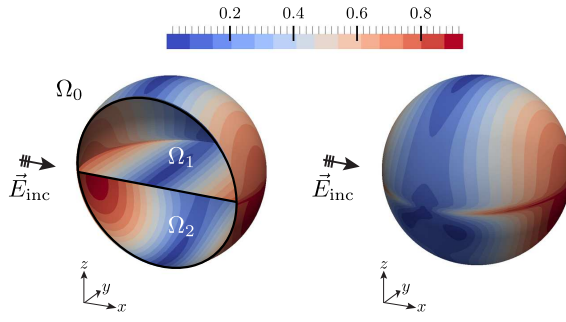


Fig. 6.1: Geometry for Experiment I. Shown is the amplitude of the imaginary part of the electric trace of the total field \mathbf{E} , solving the electromagnetic scattering problem.

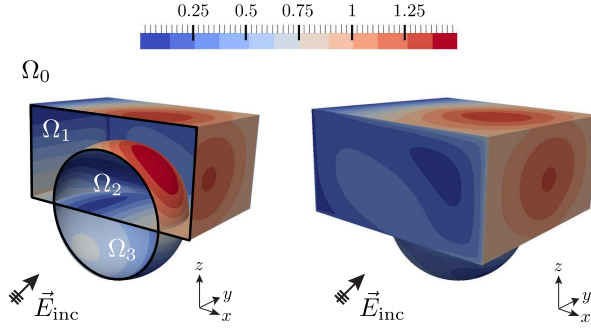


Fig. 6.2: Geometry for Experiment II. Shown is the amplitude of the imaginary part of the electric trace of the total field \mathbf{E} , solving the electromagnetic scattering problem.

Experiment II. The exciting field \mathbf{E}_{inc} is an incident plane wave with direction of propagation $\mathbf{d} = \frac{1}{\sqrt{2}}(1, 0, 1)^\top$ and the polarization vector $\mathbf{p} = (0, 1, 0)^\top$. As shown in Figure 6.2, the scatterer consists of two hemispheres Ω_2, Ω_3 with radius $\frac{1}{2}$ plus another medium occupying $\Omega_1 := \mathcal{Q} \setminus \overline{\mathcal{B}_{0.5}(\mathbf{0})}$, where $\mathcal{Q} := \{(x, y, z)^\top \in \mathbb{R}^3 : -0.7 < x < 0.7, -0.7 < y < 0.7, 0 < z < 0.7\}$. We use the wave number vector $(\kappa_0, \kappa_1, \kappa_2, \kappa_3) = (2, 3, 1, 4)$.

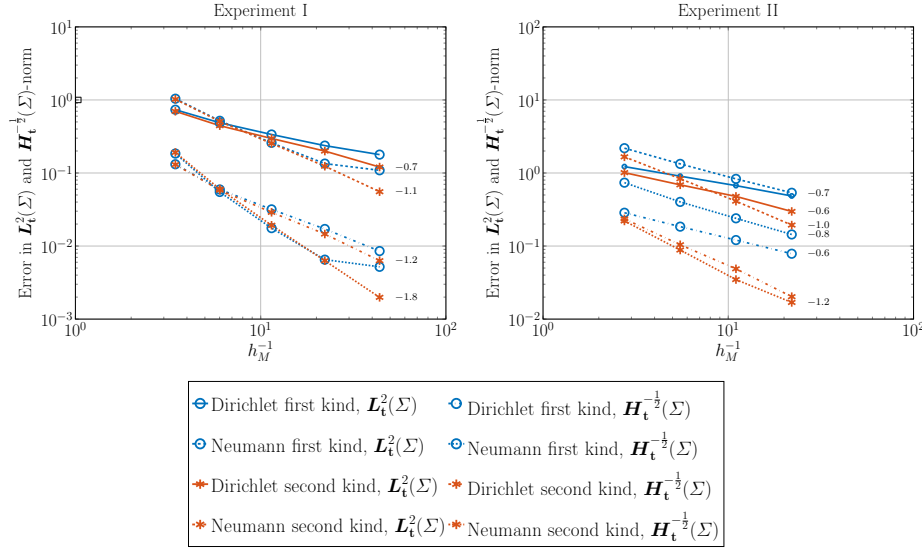


Fig. 6.3: **Convergence of the discretization error in $L_t^2(\Sigma)$ - and $H_t^{-\frac{1}{2}}(\Sigma)$ -norm** for a sequence of “uniform” triangular meshes. The error graphs are annotated with estimated rates of convergence.

6.2 Convergence of Discretization Error

By uniform refinement we create sequences of nested meshes $\{\mathcal{T}_M\}_M$ of Σ , \mathcal{T}_M comprising M flat triangular cells. The results of [35, Chapter 8] suggest that the error introduced by our polyhedral approximation of Σ will not dominate the Galerkin discretization error for trial/test spaces of piecewise constant vector fields. The global mesh width h_M of \mathcal{T}_M is the maximal diameter of its cells. We monitor the behavior of the error in $L_t^2(\Sigma)$ - and $H_t^{-\frac{1}{2}}(\Sigma)$ -norms as a function of h_M . The $H_t^{-\frac{1}{2}}(\Sigma)$ -norm is computed via the inner product $(\varphi, \nu) \mapsto \langle \gamma_{el}^i \mathbf{V}_i[0] \varphi, \bar{\nu} \rangle_{\partial \Omega_i}$, where $\mathbf{V}_i[0]$ was defined in (2.5). The equivalence of norms follows from continuity properties and the ellipticity of $\gamma_{el}^i \mathbf{V}_i[0]$ in $H_t^{-\frac{1}{2}}(\Sigma)$, shown for instance in [7, Proposition 2]. As a *reference solution* we use the discrete solution calculated with the second-kind formulation on a mesh obtained by one more step of refinement. In order to calculate the error $H_t^{-\frac{1}{2}}(\Sigma)$ -norm, we project the first-kind approximation onto the space of piecewise constant vector fields.

We use $M \in \{44, 176, 704, 2816, 11264, 45056\}$ for Experiment I, and $M \in \{140, 560, 2240, 8960, 35840\}$ for Experiment II, respectively. The various estimated errors are plotted in Fig. 6.3 and indicate algebraic convergence

⁵ The meshes were generated with GMSH [21] and for visualization of the computed data (see Figures 6.1 and 6.2) we used PARAVIEW [1].

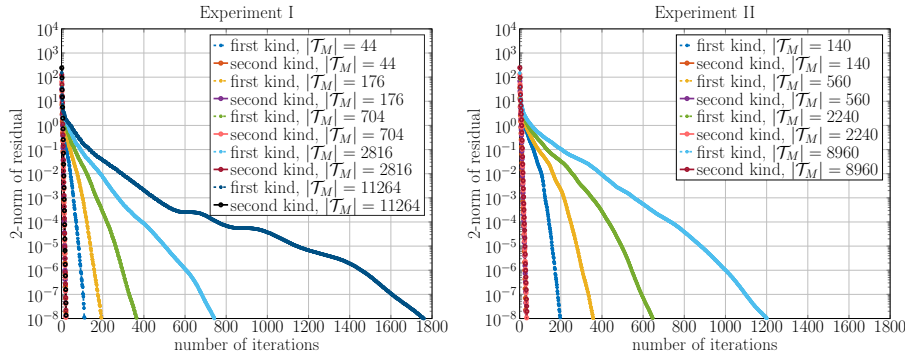


Fig. 6.4: **Convergence history of GMRES** applied to diagonally scaled first and second-kind Galerkin systems. The reddish colors correspond to the results for the second-kind system.

of the Galerkin solutions for both traces in all norms. Rates are difficult to predict due to the presence of strong edge singularities of the fields. In both experiments we observe that the accuracy of the second-kind results matches that of the first-kind results.

6.3 Convergence of GMRES and Conditioning

Figure 6.4 displays the convergence history of the GMRES iterative solver when applied to the linear systems arising from the Galerkin discretization of first-kind and second-kind BIE for the two experimental setups. As initial guess the vector $\mathbf{x}_0 = (1, \dots, 1)^\top$ is used. We observe that GMRES convergence for the second-kind system

- does not deteriorate on fine meshes,
- and is consistently significantly faster than for the first-kind system.

In order to study the dependence of the convergence of GMRES on wave numbers we fix two of them in the setting of Experiment I and vary the third, tracking the number of GMRES iterations required for a reduction of the residual \mathbf{r}_0 by six orders of magnitude in the process. Concretely, for $\kappa_1 = 10$, $\kappa_2 = 1$, we consider $\kappa_0 \in \{2.5, 5, 7.5, 10, 12.5, 15, 17.5, 20, 22.5, 25\}$, and for $\kappa_0 = 10$, $\kappa_2 = 1$, we choose $\kappa_1 \in \{2.5, 5, 7.5, 10, 12.5, 15, 17.5, 20, 22.5, 25\}$. Again, throughout, the number of required iterations is substantially smaller for the second-kind Galerkin system compared to that for the first-kind approach. In both cases we observe a very similar pronounced dependence of the number of iterations on the wave number, which hints that it may be caused by an underlying physical instability.

Though the convergence of GMRES is not directly determined by the conditioning of a linear system [3], we also plot the Euclidean condition numbers

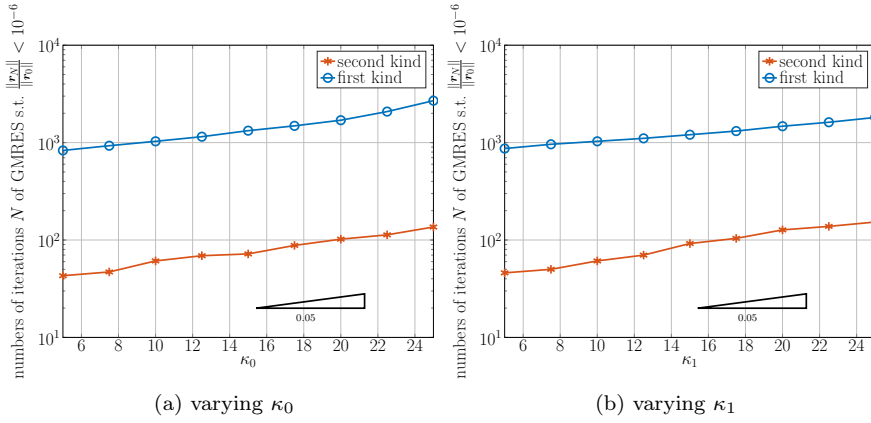


Fig. 6.5: **Convergence of GMRES for varying wave numbers** for the first and second-kind Galerkin systems for Experiment I.

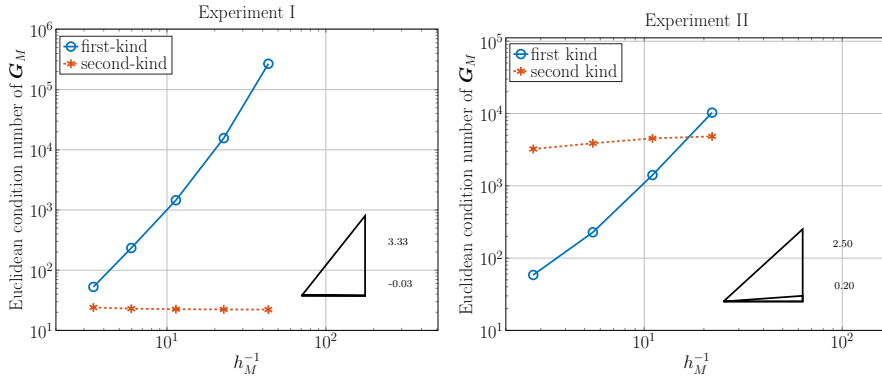


Fig. 6.6: **Euclidean condition numbers of diagonally rescaled Galerkin matrices** for a sequence of meshes.

of several (diagonally scaled) Galerkin matrices with respect to the mesh size in Figure 6.6.

We observe that the conditioning of the second-kind matrices is independent of the mesh width, whereas for the first-kind Galerkin matrices the condition numbers grow like roughly like $O(h_M^{-2})$. Admittedly, the condition numbers of the second-kind matrices can be rather large, nevertheless. They will also strongly depend on the wave numbers and the geometry.

The spectrum of the system matrix, in particular its separation from 0, is more relevant for predicting GMRES convergence. Therefore, in Figure 6.7 we plot the spectra of the (diagonally scaled) Galerkin matrices in the complex plane. We see that the spectra of the second-kind Galerkin matrices are clus-

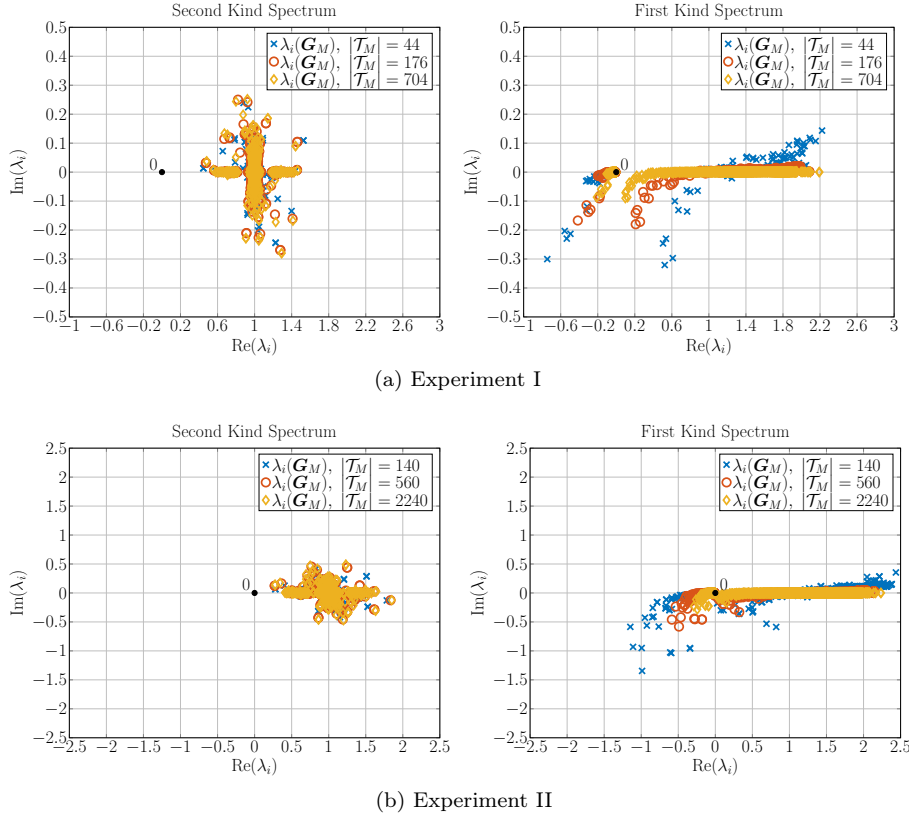


Fig. 6.7: **Distribution of the spectrum:** The eigenvalues λ_i of the (diagonally rescaled) first-kind (right plot) and second-kind (left plot) Galerkin matrices are plotted in the complex plane for a sequence of meshes.

tered around 1 and well separated from 0, while the spectra of the first-kind Galerkin matrices form clouds around 0.

7 Conclusion

We derived a new second-kind boundary integral equation (BIE) formulation for electromagnetic scattering at penetrable composite objects. Though its rigorous theoretical analysis is still incomplete, its Galerkin boundary element discretization (BEM) performs well in numerical tests. Firstly, it delivers about the same accuracy as a popular first-kind BIE approach. Secondly, it gives rise to linear systems of equations for which GMRES enjoys fast and mesh-independent convergence, on fine meshes considerably faster than for first-kind Galerkin BEM. Dependence on wave numbers persists, however.

References

1. U. Ayachit. *The ParaView Guide: A Parallel Visualization Application*. Kitware, 2015.
2. M. Bebendorf. Approximation of boundary element matrices. *Numer. Math.*, 86(4):565–589, 2000.
3. B. Beckermann, S. A. Goreinov, and E. E. Tyrtysnikov. Some remarks on the Elman estimate for GMRES. *SIAM J. Matrix Anal. Appl.*, 27(3):772–778, 2005.
4. A. Buffa. Trace theorems on non-smooth boundaries for functional spaces related to Maxwell equations: an overview. In *Computational electromagnetics (Kiel, 2001)*, volume 28 of *Lect. Notes Comput. Sci. Eng.*, pages 23–34. Springer, Berlin, 2003.
5. A. Buffa. Remarks on the discretization of some noncoercive operator with applications to heterogeneous Maxwell equations. *SIAM J. Numer. Anal.*, 43(1):1–18 (electronic), 2005.
6. A. Buffa and P. Ciarlet, Jr. On traces for functional spaces related to Maxwell’s equations. II. Hodge decompositions on the boundary of Lipschitz polyhedra and applications. *Math. Methods Appl. Sci.*, 24(1):31–48, 2001.
7. A. Buffa, M. Costabel, and C. Schwab. Boundary element methods for Maxwell’s equations on non-smooth domains. *Numer. Math.*, 92(4):679–710, 2002.
8. A. Buffa, M. Costabel, and D. Sheen. On traces for $\mathbf{H}(\mathbf{curl}, \Omega)$ in Lipschitz domains. *J. Math. Anal. Appl.*, 276(2):845–867, 2002.
9. A. Buffa and R. Hiptmair. Galerkin boundary element methods for electromagnetic scattering. In *Topics in computational wave propagation*, volume 31 of *Lect. Notes Comput. Sci. Eng.*, pages 83–124. Springer, Berlin, 2003.
10. A. Buffa, R. Hiptmair, T. von Petersdorff, and C. Schwab. Boundary element methods for Maxwell transmission problems in Lipschitz domains. *Numer. Math.*, 95(3):459–485, 2003.
11. Y. Chang and R. F. Harrington. A surface formulation for characteristic modes of material bodies. *Antennas and Propagation, IEEE Transactions on*, 25(6):789–795, 1977.
12. X. Claeys. A single trace integral formulation of the second kind for acoustic scattering. Technical Report 2011-14, Seminar for Applied Mathematics, ETH Zürich, 2011.
13. X. Claeys and R. Hiptmair. Electromagnetic scattering at composite objects: a novel multi-trace boundary integral formulation. *ESAIM Math. Model. Numer. Anal.*, 46(6):1421–1445, 2012.
14. X. Claeys, R. Hiptmair, and C. Jerez-Hanckes. Multitrace boundary integral equations. In *Direct and inverse problems in wave propagation and applications*, volume 14 of *Radon Ser. Comput. Appl. Math.*, pages 51–100. De Gruyter, Berlin, 2013.
15. X. Claeys, R. Hiptmair, C. Jerez-Hanckes, and S. Pintarelli. Novel multitrace boundary integral equations for transmission boundary value problems. In *Unified transform for boundary value problems*, pages 227–258. SIAM, Philadelphia, PA, 2015.
16. X. Claeys, R. Hiptmair, and E. Spindler. Second-kind boundary integral equations for scattering at composite partly impenetrable objects. Technical Report 2015-19, Seminar for Applied Mathematics, ETH Zürich, 2015.
17. X. Claeys, R. Hiptmair, and E. Spindler. A second-kind Galerkin boundary element method for scattering at composite objects. *BIT*, 55(1):33–57, 2015.
18. R. Coifman, V. Rokhlin, and S. Wandzura. The fast multipole method for the wave equation: a pedestrian prescription. *IEEE Antennas and Propagation Magazine*, 35(3):7–12, 1993.
19. D. Colton and R. Kress. *Inverse acoustic and electromagnetic scattering theory*, volume 93 of *Applied Mathematical Sciences*. Springer, New York, third edition, 2013.
20. M. Costabel, M. Dauge, and S. Nicaise. Singularities of Maxwell interface problems. *M2AN Math. Model. Numer. Anal.*, 33(3):627–649, 1999.
21. C. Geuzaine and J.-F. Remacle. Gmsh: A 3-d finite element mesh generator with built-in pre- and post-processing facilities. *International Journal for Numerical Methods in Engineering*, 79(11):1309–1331, 2009.
22. L. Greengard and J.-Y. Lee. Stable and accurate integral equation methods for scattering problems with multiple material interfaces in two dimensions. *J. Comput. Phys.*, 231(6):2389–2395, 2012.

23. C. Hazard and M. Lenoir. On the solution of time-harmonic scattering problems for Maxwell's equations. *SIAM J. Math. Anal.*, 27(6):1597–1630, 1996.
24. R. Hiptmair. Coupling of finite elements and boundary elements in electromagnetic scattering. *SIAM J. Numer. Anal.*, 41(3):919–944, 2003.
25. R. Hiptmair. Operator preconditioning. *Comput. Math. Appl.*, 52(5):699–706, 2006.
26. R. Hiptmair and L. Kielhorn. BETL–A generic boundary element template library. Technical Report 2012-36, Seminar for Applied Mathematics, ETH Zürich, Switzerland, 2012.
27. P. Meury. *Stable finite element boundary element Galerkin schemes for acoustic and electromagnetic scattering*. PhD thesis, ETH Zürich, 2007. ETH Diss No 17320, Prof. Dr. Ralf Hiptmair.
28. D. Mitrea, M. Mitrea, and J. Pipher. Vector potential theory on nonsmooth domains in \mathbf{R}^3 and applications to electromagnetic scattering. *J. Fourier Anal. Appl.*, 3(2):131–192, 1997.
29. I. Mitrea and K. Ott. Spectral theory and iterative methods for the Maxwell system in nonsmooth domains. *Math. Nachr.*, 283(6):784–804, 2010.
30. P. Monk. *Finite element methods for Maxwell's equations*. Numerical Mathematics and Scientific Computation. Oxford University Press, New York, 2003.
31. C. Müller. *Foundations of the mathematical theory of electromagnetic waves*. Revised and enlarged translation from the German. Die Grundlehren der mathematischen Wissenschaften, Band 155. Springer-Verlag, New York-Heidelberg, 1969.
32. J.-C. Nédélec. *Acoustic and electromagnetic equations*, volume 144 of *Applied Mathematical Sciences*. Springer-Verlag, New York, 2001. Integral representations for harmonic problems.
33. A. J. Poggio and E. K. Miller. *Computer techniques for electromagnetics: Chapter 4: Integral equation solutions of three-dimensional scattering problems*. Pergamon Press, Oxford-New York-Toronto, Ont., 1973. Computer Techniques for Electromagnetics, Vol. 7.
34. V. Rokhlin. Rapid solution of integral equations of scattering theory in two dimensions. *J. Comput. Phys.*, 86(2):414–439, 1990.
35. S. A. Sauter and C. Schwab. *Boundary element methods*, volume 39 of *Springer Series in Computational Mathematics*. Springer-Verlag, Berlin, 2011. Translated and expanded from the 2004 German original.
36. E. Spindler. *Second Kind Single-Trace Boundary Integral Formulations for Scattering at Composite Objects*. PhD thesis, ETH Zürich, 2016. ETH Diss No 23620, Prof. Dr. Ralf Hiptmair.
37. O. Steinbach and W. L. Wendland. The construction of some efficient preconditioners in the boundary element method. *Adv. Comput. Math.*, 9(1-2):191–216, 1998. Numerical treatment of boundary integral equations.
38. R. H. Torres. A transmission problem in the scattering of electromagnetic waves by a penetrable object. *SIAM J. Math. Anal.*, 27(5):1406–1423, 1996.
39. T.-K. Wu and L. L. Tsai. Scattering from arbitrarily-shaped lossy dielectric bodies of revolution. *Radio Science*, 12(5):709–718, 1977.
40. P. Ylä-Oijala and M. Taskinen. Well-conditioned Müller formulation for electromagnetic scattering by dielectric objects. *IEEE Trans. Antennas and Propagation*, 53(10):3316–3323, 2005.